Title: Inflammation and matrix metalloproteinase 9 (Mmp-9) regulate photoreceptor regeneration in the adult zebrafish

Authors: Nicholas Silva[1, 2], Mikiko Nagashima[2], Jingling Li[3], Laura Kakuk-Atkins[2], Milad Ashrafzadeh[2], David R. Hyde[3], Peter F. Hitchcock[1, 2]

1. Neuroscience Graduate Program, University of Michigan, Ann Arbor, MI 48109
2. Department of Ophthalmology and Visual Sciences, University of Michigan, Ann Arbor, MI 48105
3. Department of Biological Sciences, University of Notre Dame, Notre Dame, IN, 46556

Corresponding Author:

Peter F. Hitchcock
University of Michigan
Department of Ophthalmology and Visual Sciences
W.K. Kellogg Eye Center
1000 Wall Street
Ann Arbor, MI 48105
peterh@med.umich.edu
734-763-8169

Abstract

Brain injury activates complex inflammatory signals in dying neurons, surviving neurons, and glia. Here, we establish that inflammation regulates the regeneration of photoreceptors in the zebrafish retina and determine the cellular expression and function of the inflammatory protease, matrix metalloproteinase 9 (Mmp-9), during this regenerative neurogenesis. Anti-inflammatory treatment suppresses both the number of injury-induced progenitors and regenerated photoreceptors. Following photoreceptor injury and death, *mmp-9* is expressed in Müller glia, the intrinsic retinal stem cell, and Müller glia-derived photoreceptor progenitors. Deleting *mmp-9* results in over production of injury-induced progenitors and regenerated photoreceptors, but over time the absence of Mmp9 compromises the maturation and survival of the regenerated cones. Anti-inflammatory treatment in mutants rescues the defects in cone maturation and survival. These data provide a link between injury-induced inflammation in the vertebrate CNS, Mmp-9 function during photoreceptor regeneration and the requirement of Mmp9 for the survival of regenerated cones.

Introduction

Inflammation modulates immune and nonimmune functions during tissue development, repair, and diseases (Deverman and Patterson, 2009; Ekdahl et al., 2009). Acute inflammation involves the secretion of proinflammatory cytokines and chemokines that recruit immune cells to the damaged tissue (Liddiard et al., 2011; Nathan, 2002). In the adult central nervous system of mammals, acute inflammation can activate signaling cascades in stem and progenitor cells that stimulate neurogenic proliferation and promote neurogenesis (Borsini et al., 2015; Ekdahl et al., 2009; Kizil et al., 2015; Kyritsis et al., 2014, 2012). Chronic inflammation, however, is detrimental, and results in secondary damage to neurons and, in severe cases, neurodegenerative diseases (Amor et al., 2010). Proper regulation of the inflammatory cascades in the central nervous system is critical both to maintain tissue homeostasis and successfully repair injuries.

Unlike mammals, which possess a limited capacity for tissue regeneration, zebrafish have an astonishing ability to regenerate tissues and organs, such as fins, heart, brain, and retina (Gemberling et al., 2013; Kizil et al., 2012; Lenkowski and Raymond, 2014). Studies using zebrafish have identified cellular and molecular mechanisms which may unlock the regenerative potential of mammalian tissues (Ueki et al., 2015). Such mechanisms include inflammation. In zebrafish acute inflammation is both necessary and sufficient to induce neuronal regeneration (Kyritsis et al., 2012).

In the retina of zebrafish, Müller glia serve as intrinsic stem cells, supporting the ability to regenerate all types of retinal neurons (Bernardos et al., 2007; Fausett and Goldman, 2006). In response to neuronal injury and death, Müller glia undergo transient gliotic response, followed by partial dedifferentiation and entry into the cell cycle. Müller glia then undergo a single asymmetrical division to produce multipotent progenitors, which rapidly proliferate, migrate to areas of neuronal loss and differentiate into the original collection of depleted neurons (Fimbel et al., 2007; Sherpa et al., 2008; Goldman, 2014; Gorsuch and Hyde, 2014; Lenkowski and

Raymond, 2014). In contrast, in the mammalian retina, neuronal death leads to persistent active gliosis in Müller glia and failure of the spontaneous expression of intrinsic reprogramming factors. This limits the ability for neuronal regeneration (Bringmann et al., 2009, 2006; Reichenbach and Bringmann, 2013; see also Ueki et al., 2015). In the zebrafish retina, paracrine and autocrine signaling that engage Müller glia plays a pivotal role facilitating regenerative neurogenesis (Nelson et al., 2013; Zhao et al., 2014). Following a photolytic lesion, dying photoreceptors secrete Tnf-α, which signals to Müller glia, which then respond by partial dedifferentiation, and synthesis of Tnf–α and entery into the cell cycle (Nelson et al., 2013). Mechanical lesions induce the expression of *leptin* and Il-6 family cytokines in Müller glia and progenitors and is required for injury-induced proliferation (Zhao et al., 2014).

Matrix metalloproteinase 9 (Mmp-9) is a secreted protease that plays a prominent role in proliferation, migration, and differentiation by remodeling extracellular molecules, including adhesion molecules, growth factors and cytokines (Bonnans et al., 2014; Le et al., 2007; Masure et al., 1991; Parks et al., 2004; Vandooren et al., 2014, 2013b). In adult tissues, Mmp-9 is dramatically induced following various types of injuries (Vandooren et al., 2014, 2013b). During heart regeneration in zebrafish, Mmp-9 induced in cardiac fibroblasts recruits leukocytes via activating chemokines and, thereby, regulates cardiac regeneration (Xu et al., 2018). In the nervous system, inflammatory cytokines, such as Tnf–α and Il-1β, activate *mmp-9* expression following injury (Shubayev et al., 2006; Vecil et al., 2000). However, the cellular expression and function of Mmp-9 are complicated, and the role Mmp-9 plays during tissue regeneration is likely tissue, substrate and injury context dependent (Hindi et al., 2013; Vandooren et al., 2014b; Ando et al., 2017; Xue et al., 2017). The cellular expression and function of Mmp-9 during photoreceptor regeneration in the zebrafish are unknown.

In the current study, we determine the general role of inflammation and the cellular expression and function of the matrix metalloproteinase, Mmp-9, during photoreceptor

regeneration. We establish that inflammation positively governs the proliferation of Müller glia and Müller glia-derived progenitors. We show that *mmp-9* is expressed in Müller glia as they prepare to enter the cell cycle and Müller glia-derived progenitors. *Mmp-9* is down regulated as these cells exit the cell cycle. Using a loss-of-function mutant, we determine that Mmp-9 negatively regulates the proliferation of Müller glia-derived progenitors. Finally, we demonstrate that following photoreceptor regeneration, Mmp-9 is required for the maturation and survival of regenerated cone photoreceptors.

RESULTS

Inflammatory genes are strongly induced during photoreceptor regeneration

To characterize the inflammatory response during photoreceptor regeneration, qPCR was used to quantify the expression of a subset of inflammatory genes, *mmp-9, tnf-α*, *tnf-β*, *il-8, nfκb1,* and *nfκb2*, previously shown to regulate various forms of tissue regeneration in zebrafish (de Oliveira et al., 2013; LeBert et al., 2015; Nelson et al., 2013; Karra et al., 2015). The time course of gene expression follows closely the well-established time course for the injury response in Müller glia, the appearance of the Müller glia-derived progenitors, and the subsequent differentiation of regenerated photoreceptors (Figure 1A; see (Gorsuch and Hyde, 2014)). Upregulation of gene expression is detectable by 8 hours post lesion (hpl), and the rising phase in expression corresponds to the interval when Müller glia prepare to enter the cell cycle. Expression levels then slowly decline as the Müller glia-derived photoreceptor progenitors divide, migrate to the outer nuclear layer and differentiate into regenerated photoreceptors (168 hpl; Figure 1A). Interestingly, among these genes, *mmp-9* shows the highest levels of expression, which is maximal at 48 hpl. Further, by 168 hpl *mmp-9* levels are reduced to only about 70% of the peak value (ANOVA F-ratio = 22.23, p= .0001; Figure 1A). The pro-inflammatory cytokine, Tnf-α, has been posited to be responsible for initiating photoreceptor regeneration in zebrafish (Gorsuch and Hyde, 2014; Nelson et al., 2013), but at all time points in this assay, the levels of *tnf-α* expression were not significantly different from controls. Our assay for *tnf-α* failed to replicate previous results (Nelson et al., 2013), and we infer this is most likely a consequence of a potential technical issues, perhaps reflecting the different assays used here and in Nelson et al. (2013) to detect *tnf-α*. Nonetheless, these data show that in zebrafish a photolytic lesion, which leads to photoreceptor death, induces rapid expression of characteristic inflammatory genes that follows a time course reflecting the well-described events that underlie

photoreceptor regeneration. Further, the expression of *mmp-9* remains significantly elevated as photoreceptor differentiation commences.

Inflammation regulates injury-induced proliferation and photoreceptor regeneration

To determine if inflammation regulates aspects of photoreceptor regeneration, the glucocorticoid steroid, dexamethasone (Dex), was used to suppress the inflammatory response (see, Kyritsis et al., 2012). To validate the effectiveness of the Dex treatment, the expression levels of inflammatory genes were quantified in control and Dex-treated groups. At 72 hpl, the expression of *mmp-9*, *il-6*, and *nfκb1* were significantly decreased following dexamethasone treatment (p values = .0001, .0061, .0003, respectively; Supplemental Figure 1). Dex treatment did not suppress the expression of *tnf-a*, which was expected, given this gene was not significantly induced in the original assay. The reasons for the failure of the Dex treatment to suppress *il-8* expression are unresolved.

Based on previous results (Kyritsis et al., 2012), assays of cell proliferation and photoreceptor regeneration were performed for control animals and animals treated with Dex. Dividing cells were labelled with BrdU between 24 and 48 hpl to mark progenitors that will give rise to regenerated photoreceptors, and regenerated photoreceptors were identified as BrdU-labeled nuclei in the outer nuclear layer surrounded by *in situ* hybridization signal for either *rho* (rods) or *pde6c* (cones). At 72 hpl (Figure 1B, Methods), there was significantly fewer BrdU-labeled cells in Dex-treated retinas compared to controls (p= 0.0079; Figure 1C, D). Similarly, at 7 days post lesion (dpl) there were significantly fewer regenerated rods and cones, in Dex-treated groups compared to controls (Figure 2B, C; p=0.0012). These results indicate that, consistent with data showing the requirement for inflammation in neuronal regeneration in the forebrain of zebrafish (Kyritsis et al., 2012), inflammatory mechanisms also promote photoreceptor regeneration in the retina. Further, in the zebrafish central nervous system inflammation positively regulates the proliferation that underlies neuronal regeneration, a key step in quantitatively determining the number of regenerated neurons.

Müller glia and Müller glia-derived progenitors express *mmp-9*

Due to the varied roles played by *mmp-9* in injured/regenerating tissues (Vandooren et al., 2014), and its persistent expression throughout the time-course of photoreceptor regeneration (Figure 1A), the specific function of Mmp-9 was investigated further. *In situ* hybridization was performed first, to identify the cellular patterns of expression of *mmp-9*. This was performed using the Müller glia reporter line, *Tg[gfap:EGFP]mi2002,* and BrdU labeling of dividing cells 24 hrs prior to sacrifice. There is no detectable expression of *mmp-9* in unlesioned retinas. In contrast, by 24 hpl, *mmp-9* is expressed exclusively in Müller glia*,* but at a time-point prior to their entry into S-phase of the cell cycle (Figure 3A). By 48 hpl, ~97% of BrdU-labeled Müller glia express *mmp-9* (Figure 3A, B, C). At 72 hpl, the expression of *mmp-9* decreases (Figure 3A, C), and the cellular expression shifts to the Müller glia-derived progenitors, as evidenced by the absence of dGFP in BrdU-labeled cells that express *mmp-9* (Figure 3A). These data suggest that *mmp-9* is expressed in the subset of Müller glia that will enter the cell cycle in response to photolytic lesion and the photoreceptor progenitors originating from these cells.

Mmp-9 protein is present and catalytically active following photoreceptor death

In tissues, Mmp-9 is synthesized and secreted in a pro-form, as a zymogen, then converted into an active protease (Chattopadhyay and Shubayev, 2009; Vandooren et al., 2013a). Western blot analysis was used to characterize the induction of protein synthesis and zymogram assays were used to determine the time course of protein synthesis and catalytic activity for Mmp-9 during photoreceptor regeneration (Vandooren et al., 2013a, 2013b). Mmp-9 is not detected in unlesioned retinas, consistent with the qRT-PCR and *in situ* hybridization data (Figure 1A, 3A, 4A). At 16 hpl, the first time point sampled, the un-cleaved, pro-form of Mmp-9 is detected as an upper band in Western blots (Figure 4A). Mmp-9 levels peak by 24 hpl, and both forms of Mmp-9 are detected. Mmp-9 levels decrease between 24 and 72 hpl, and during this interval the protein mostly appears in a slightly lower band, consistent with the active form of the

protein. Mmp-9 levels are undetectable by Western blot analysis at 5 dpl (ANOVA F-ratio = 8.377, p =.0013) (Figure 4 A, B). To evaluate the catalytic activity of Mmp-9, the same protein samples as were used for the Western blot analysis were used for the zymogram analysis (Chattopadhyay and Shubayev, 2009; Vandooren et al., 2013a). Recombinant, active human MMP-9 was used as a positive control and shows strong catalytic activity as evidenced by the large negatively stained band. Unlesioned retinas contain no Mmp-9 catalytic activity. In contrast, and as would be predicted, the catalytic activity parallels the data from the Western blot analysis (ANOVA F-ratio = 11.870, p = .0003) (Figure 4C, D). Together, results from the Western blot and zymogram analyses show that catalytically-active Mmp-9 is induced by a lesion that selectively injures photoreceptors, and the time course of Mmp-9 synthesis and catalytic activity parallels the proliferative phases of photoreceptor regeneration. It is noteworthy that the peak of protein synthesis and catalytic activity is at 24hpl, which precedes the peak of mRNA synthesis (cf. Figures 4 and 1A), suggesting independent regulation of *mmp-9* transcription and translation.

Tnf-α is sufficient to induce *mmp-9* expression in unlesioned retinas

Tnf-α induces *mmp-9* expression in a variety of tissues (Vandooren et al., 2014). In zebrafish, this cytokine is induced by death of photoreceptors and inner retinal neurons, and it is required for Müller glia to enter the cell cycle (Nelson et al., 2013). Therefore, the ability of Tnf-α to induce *mmp-9* expression in the zebrafish retina was tested. Either Tnf-α or the elution buffer used to column purify Tnf-α was injected into the vitreous space of unlesioned eyes, and *mmp-9* expression was quantified by qRT-PCR (Figure 5A). There was no induction of *mmp-9* in eyes that were either uninjected or eyes injected with elution buffer only. In contrast, *mmp-9* was strongly induced in the retinas of eyes that received intraocular injections of Tnf-α (p = 0.0229) (Figure 5B). *stat-3*, which serves as a positive control for injury-induced proliferation in the retina (Nelson et al., 2012) was also strongly induced by Tnf-α injections (p = 0.0344) (Figure 5C).

These results indicate that Mmp-9 functions downstream of Tnf-α following photoreceptor injury and death.

CRISPR mutants lack Mmp-9 protein and catalytic activity

To investigate the function of *mmp-9* during photoreceptor regeneration, mutants were generated using CRISPR-Cas9 (Hwang et al., 2013), targeted to the *mmp-9* catalytic domain in exon 2 (Figure 6A). The 19 base sgRNA produced several alleles, two of which were bred to homozygosity and characterized further (Figure 6B). Individuals from the two mutant lines were crossed to create compound heterozygotes to evaluate the potential effects off target effects in the two independent lines (see next section). The two *mmp-9* lines carry mutations that each results in a frameshift that gives rise to predicted premature stop codons (Supplemental Figure 2). Retinas from mutants were characterized by Western blot analysis and zymogram assays. Unlesioned retinas had no detectable Mmp-9 or catalytic activity (Figure 6C, D). As expected, following a photolytic lesion, Mmp-9 protein and catalytic activity are present in wild-type retinas (Figure 6C, D). In contrast, there was only trace Mmp-9 and catalytic activity in the retinas of mutants carrying the 8bp insertion, and no detectable Mmp-9 or catalytic activity in the retinas carrying the 23bp deletion (Figure 6 C, D). Based on these results, all subsequent experiments were conducting using the 23bp deletion mutant, though the basic observations reported here were confirmed in the 8bp insertional mutant (data not shown) and the compound heterozygotes (see below).

Photoreceptor death results in overproduction of photoreceptor progenitors and regenerated photoreceptors

We first sought to determine if there were any differences in the starting points for the injury-induced proliferation in the *mmp-9* mutants. Therefore, we compared the number of Müller glia and the number of mitotic progenitors, which support persistent neurogenesis (Raymond et al., 2006), in wild-type and mutant retinas. This analysis showed that there were no differences between wild-type and mutants in the number of Müller glia or the level of

intrinsic cell proliferation (Supplemental Figure 3A, B). To determine the consequence of Mmp-9 loss-of-function on retinal regeneration, wild-type and mutant animals received photolytic lesions, Müller glia-derived photoreceptor progenitors were labeled with BrdU between 48-72 hpl, and BrdU-labeled cells were counted at 72 hpl. Relative to wild-type animals, mutants had significantly more BrdU-labeled progenitors at 72 hpl ($p = .0186$) (Figure 7A, B). This over production of injury-induced progenitors was also observed in the 8bp insertional mutant (data not shown) and the compound heterozygotes (Supplemental Figure 3C), confirming that the hyperproliferation can be ascribed solely to Mmp-9 loss-of-function.

It is also well established that Mmp-9 can modulate cell migration (Parks et al., 2004). To determine if Mmp-9 loss-of-function alters migration of photoreceptor progenitors from the inner nuclear layer, where Müller glia reside, to the outer nuclear layer, which exclusively contains photoreceptor nuclei, animals were subjected to photolytic lesions, exposed to BrdU between 48 and 72hpl and allowed to survive to 7 days post lesion (dpl), a time point where proliferation and migration are complete and photoreceptor differentiation has commenced. Qualitative inspection shows that Mmp-9 loss-of-function does not alter the migration of photoreceptor progenitors (Figure 7A, C). Further, cell counts showed that the over production of photoreceptor progenitors observed in mutants at 72hpl results in significantly more BrdU-labeled cells within the ONL at 7 dpl ($p = .0001$; Figure 7B, D), and a significantly more regenerated rod and cone photoreceptors ($p = .0301$ and $p = .0005$, respectively; Figure 7 E-G). Together, these data show that, in the absence of an injury, Mmp-9 loss-of-function has no impact on early retinal development, the proliferative potential of the adult retina or migration of progenitor cells across retinal and synaptic layers. However, the hyperproliferation of injury-induced progenitors in mutants shows that Mmp-9 functions to negatively regulate proliferation of Müller glia-derived progenitors, though the mechanisms through which this is accomplished are not yet known (see Discussion).

Mmp-9 governs maturation and survival of regenerated cone photoreceptors

The qPCR data showed that *mmp-9* levels remain significantly elevated at the time injury-induced photoreceptor progenitors exit the cell cycle and begin differentiating into mature photoreceptors (Figure 1A). This suggested that Mmp-9 may have functional roles beyond regulating proliferation during the initial stages of photoreceptor regeneration. Therefore, regenerated rod and cone photoreceptors were qualitatively and quantitatively compared in wild-type and mutants at 21dpl, a time point where regeneration is complete (Powell et al., 2016). For both groups, retinal sections were labeled with rod- and cone-specific antibodies and regenerated photoreceptors were counted in sections and whole mount preparations. These analyses showed there were no qualitative differences between wild-type and mutants in the appearance of regenerated rod photoreceptors (Figure 8A), and the initial over production of rod photoreceptors observed at 7dpl was present at 21dpl (Figure 8B, C).

However, at 21dpl, the maturation and survival of cones in mutant retinas were clearly compromised. Relative to controls, regenerated cones in mutants have shorter outer segments and appear to be fewer in number (Figure 8A, inset 8B, 8C). Counts of regenerated cones in tissues sections show the initial over production of cones, evident at 7 dpl, is absent (Figure 8C). Cones were also counted in retinal wholemounts (Figure 9). In the wholemounts, cones were identified by their prominent profiles in optical sections taken through the inner segments, visible when retinas are stained with an antibody against the tight junction protein, ZO-1 (Nagashima et al., 2017). In both wild-type and mutant retinas, cone photoreceptors in unlesioned retinas are characterized by the very precise lattice mosaic, a feature of cone photoreceptors in teleost fish (Nagashima et al., 2017; Figure 9A). Following photoreceptor regeneration, areas of the retina that contain regenerated photoreceptors are readily identifiable by the marked spatial degradation of the mosaic, though individual cone photoreceptors are remain readily identifiable (Nagashima et al., 2017). Counts of regenerated cones in whole mounts show that mutants have significantly fewer regenerated cones than wildtype animals ($p=.0229$) (Figure 9A, B). Finally, as an independent measure of the maturation of cone

photoreceptors, Western blot analysis was performed using an antibody against the cone-specific transducin protein, Gnat-2 (Figure 9C; Lagman et al., 2015). As expected, Gnat-2 levels in unlesioned retinas are comparable in wild-type and mutant animals. In lesioned retinas, Gnat-2 levels begin to recover in wild-type animals by 14 dpl, and by 21 dpl values in wild-type animals are nearly at the levels found in unlesioned retinas (Figure 9C, D). In contrast, Gnat-2 levels in mutants lag behind wild-type levels, and at 21dpl Gnat-2 levels in mutant animals are significantly less than in wild-types ($p = .0014$) (Figure 9C, D). Comparable measures specific to rod photoreceptors showed there were no differences between wild-type and mutant animals (data not shown). Together, these results show that Mmp-9 also has a functional role during photoreceptor regeneration, well after injury-induced proliferation and the initial differentiation of regenerated photoreceptors. Further, this function is specific to cone photoreceptors and the maturation and survival of these cells.

Late anti-inflammatory treatment rescues the maturation and survival defect of regenerated cones in *mmp-9* mutants

MMP-9 is known to cleave inflammatory cytokines and may function to resolve tissue inflammation. To determine if prolonged inflammation in the *mmp-9* mutants produces the defects in the maturation and survival of cone photoreceptors, we treated mutants with vehicle or Dex between 3 and 13dpl to suppress the inflammatory response after the formation of Müller glia-derived progenitors and during photoreceptor differentiation (Figure 10A). Cone photoreceptors were then counted in retinal whole mounts at 21dpl from vehicle and Dex-treated mutants. The number of cones at 21dpl in vehicle-treated mutants approximates that shown above (Figure 9; Figure 10B). In contrast, there are significantly more regenerated cones in the Dex-treated mutants than in the vehicle-treated controls (Figure 10B,C; $p = .01$), restoring the number of regenerated cones nearly to that observed in wild-type animals. To determine if the Dex treatment also affected cone maturation, IHC was used to qualitatively evaluate photoreceptor morphology as a readout of maturation. The regenerated cones in the Dex-

treated mutants noticeably more mature than in controls, as evidenced by their more regular arrangement, overall length and lengths of the outer segments (Figure 10D). Correlated with these data, activated microglia are present in the ONL of vehicle-treated mutants (Figure 10E). Together, these results suggest that the absence of Mmp9 gives rise to a persistent inflammation among the regenerated photoreceptors, which negatively impacts the maturation and survival of cone photoreceptors.

DISCUSSION

Our findings are summarized in Fig. 11. In response to photoreceptor cell death, Müller glia undergo a single asymmetric division through interkinetic nuclear migration to produce photoreceptor progenitors, which rapidly proliferate and differentiate to replace the depleted cells (Fig. 11A, B). Dexamethasone-induced immunosuppression inhibits proliferation, resulting in diminished photoreceptor regeneration (Fig. 11C). Loss of Mmp-9 function effectively reverses the consequences of immunosuppression, resulting in hyperproliferation and overproduction of regenerated photoreceptors (Fig. 11D). However, the absence of Mmp-9 leads to defects in the maturation and survival of cone photoreceptors (Fig. 11D). Immunosuppression in mutants following photoreceptor regeneration rescues the maturation and survival defects (Fig. 11E). Based on these results, we conclude that inflammation functions during the proliferative phase of photoreceptor regeneration to match the number of progenitors to the extent of the cell death. Our results indicate that Mmp-9 provides inhibitory balance that refines this proliferative response.

The response of stem cells to inflammatory signals is required for regenerative neurogenesis (Fischer et al., 2014; Kyritsis et al., 2012; White et al., 2017). In the forebrain of adult zebrafish, immunosuppression inhibits the production of progenitors after traumatic lesion (Kyritsis et al., 2012). In the zebrafish retina, immunosuppression results in decreased migration of microglia into the outer retina during the regeneration of rod photoreceptors (White et al., 2017). In the chick, ablation of microglia completely suppresses the formation of Müller glia-derived retinal progenitors (Fischer et al., 2014). Our data are consistent with these reports and demonstrate that acute inflammation is required for photoreceptor regeneration in the vertebrate retina.

In response to photoreceptor injury, *mmp-9* is rapidly induced in Müller glia, anti-inflammatory treatment significantly suppresses the *mmp-9* expression, and in unlesioned retinas the proinflammatory cytokine, Tnf-α, a proinflammatory cytokine, is sufficient to stimulate

mmp-9 expression in unlesioned retinas. This trio of results validates Mmp-9 as a component of the inflammatory response in the retina. Several previous reports showed that following neuronal death Müller glia secrete the inflammatory cytokines, *tnf-a*, *leptin*, and *il-11* (Nelson et al., 2013; Zhao et al., 2014). Recent transcriptome and gene ontology analysis for Müller glia, isolated during photoreceptor injury and death, identified cytokine signaling and the immune response as activated pathways (Roesch et al., 2012; Sifuentes et al., 2016). Our data add details to the intrinsic immune response in the retina that is required for stem cell-based regeneration of photoreceptors. It is interesting to note that in the transcriptomes of Müller glia in both zebrafish and mouse models of photoreceptor degeneration the activation of cytokine pathways is conserved (Roesch et al., 2012; Sifuentes et al., 2016), suggesting that modulating intrinsic cellular mechanisms may be a promising therapeutic avenue to regenerate retinal neurons (Vetter et al., 2017).

An intriguing observation from our study is that Mmp-9 loss-of-function mutants have an increased number of injury-induced progenitors, resulting initially in more regenerated photoreceptors. The overproduction of regenerated photoreceptors is interpreted simply to result from the overproduction of progenitors and no alterations in the timing of cell cycle exit and photoreceptor differentiation. There are at least three interpretations for the overproduction of photoreceptor progenitors. First, the absence of Mmp-9 may allow more Müller glia to enter the cell cycle. Previous studies showed that neuronal damage results in only 65-75% of the Müller glia entering the cell cycle (Nagashima et al., 2013). However, we demonstrated that *mmp-9* was expressed only by dividing Müller glia. The absence of of proliferation in *mmp-9*-negative Müller glia argues against the possibility that additional Müller glia are recruited to the cell cycle. Second, in the *mmp-9* mutants Müller glia may undergo more than a one round of cell division, thereby increasing the size of the initial pool of Müller glia-derived progenitors, which then divide at a normal rate. We do not favor this possibility, given a single asymmetric division among Müller glia is a hallmark of regenerative neurogenesis in the zebrafish retina. Third, in

the *mmp-9* mutants, proliferation of the Müller glia-derived progenitors is accelerated. We view this the likeliest of the three possibilities, and hypothesize that, as an extracellular protease, Mmp-9 regulates the concentration of cytokines and/or growth factors that regulates cell cycle kinetics within the niche of progenitors that cluster around each parental Müller glia (Bosak et al., 2018; Le et al., 2007; Manicone and Mcguire, 2008; Parks et al., 2004; Luo et al., 2012; Vandooren et al., 2013b). In the absence of Mmp-9, excess mitogenic signals lead to accelerated proliferation.

Recently, Kaur et al (2018) demonstrated a regulatory feedback loop involving Shh signaling and Mmp-9 during retinal regeneration in zebrafish. Pharmacological and genetic suppression of Shh signaling inhibited the proliferative response of Müller glia and their progenitors. This was accompanied by up-regulation of *mmp-9* and the repressor of proliferation, *insm1a* (Kaur et al., 2018; Ramachandran et al., 2012). The hyperproliferation we observed in the *mmp-9* mutants is consistent with their proposed model. When Shh signaling declines, progenitors increase secreted Mmp-9, which then degrades extracellular factors that facilitate proliferative competence, resulting in increased *insm1a* and exit from cell cycle. In this model, the absence of Mmp-9 would fail to degrade factors that stimulate proliferation, leading to hyperproliferation. The positive feedback loop between Shh signaling and Mmp-9 suggests that Shh and HB-EGB, factors that function upstream of *insm1a*, may be proteolytic substrates for the Mmp-9 (Wan et al., 2012).

An inconsistency in the Kauer et al., (2018) study is their observation that morpholino inhibition of Mmp-9 action decreases the production of Müller glia-derived progenitors. This report is inconsistent with our data from the *mmp-9* mutants and raises the possibility that the reliance on morpholinos, which have recently raised concerns regarding their potential for off-target effects (Schulte-Merker and Stainier, 2014; Kok et al., 2015), may be the origin of these inconsistent data.

In the Mmp-9 loss-of-function mutants, survival and maturation of regenerated cone photoreceptors are compromised. It is well established that chronic inflammation is a risk factor for photoreceptor dystrophies in humans, such as retinitis pigmentosa and age-related macular degeneration (AMD; Kauppinen et al., 2016; Chen and Xu, 2012; Whitcup et al., 2013; Yoshida et al., 2013). A subset of patients with AMD exhibit single nucleotide polymorphism (SNP) variants in the *MMP-9* gene, and elevated inflammation is associated with AMD pathogenesis (Fritsche et al., 2016; Kauppinen et al., 2016; Parks et al., 2004). Mutational variants in the inflammatory regulators, TIMP-3, TGFB, TNF-α were also identified in human patients with AMD (Fritsche et al., 2016). We hypothesize that during photoreceptor regeneration in zebrafish, Mmp-9 functions late to resolve the acute inflammation stimulated by death of the photoreceptors, and, in the *mmp-9* mutants, there is prolonged inflammation that is selectively damaging to cones. The *mmp-9* mutants studied here may recapitulate elements of the pathologies that are characteristic of inflammatory photoreceptor diseases in humans, including AMD. Our study begins to shed light on the functional roles of Mmp-9 in the retina and a potentially important link between intrinsic retinal immunity, human photoreceptor dystrophies and photoreceptor regeneration.

MATERIALS AND METHODS

Animals

Wild-type, AB strain zebrafish (*Danio rerio*; ZIRC, University of Oregon, Eugene, Oregon) were propagated, maintained, and housed in recirculating habitats at 28.5°C and on a 14/10-h light/dark cycle. Animals used in this study were between 6 and12 months of age. The transgenic reporter line, *Tg[gfap:EGFP]mi2002,* was used to identify Müller glia in retinal sections (Bernardos and Raymond, 2006). All experimental protocols were approved by the University of Michigan's Institutional Animal Care and Use Committee (IACUC).

Light Lesions

To kill photoreceptors, fish were dark adapted, then exposed to high intensity light (ca. 100,000 lux) for 30 minutes, followed by exposure to constant light (ca. 30.000 lux) for 72 hours (Bernardos and Raymond, 2006; Taylor et al., 2015). After 72 hours fish were returned to the recirculating habitats and normal light/dark cycle.

Reverse Transcriptase Quantitative Real-Time PCR (qRT-PCR)

Total RNA was extracted from dissected whole retinas using TRIzol (Invitrogen, Carlsbad, CA). For each time point, three independent biological replicates were collected, and each replicate contained six homogenized retinas from three fish (18 retinas/time point). Reverse transcription to cDNA was performed using 1 µg RNA (Qiagen QuantiTect Reverse Transcription kit; Venlo, Netherlands). For qPCR, each biological replicate was run in triplicate with 6 ng cDNA and Bio-Rad IQ SYBR Green Supermix (Bio-Rad CFX384 Touch Real Time PCR Detection System; Hercules, CA). Data represented as Log2 fold change was calculated using DDC_T method and normalized to the housekeeping gene, *gpia*. Primers used are listed in Table 1.

Anti-inflammatory treatment

A previously described protocol was used suppress injury-induced inflammation (Kyritsis et al., 2012). Briefly, fish were housed in system water with 15 mg/ L dexamethasone (Sigma, Ca. No: D1756) diluted in 0.1% MetOH. Dexamethasone was changed daily and fish were fed brine

shrimp every other day. Controls animals were housed in system water containing the vehicle solution.

Immunohistochemistry

Dissected eyecups were fixed overnight at 4°C in phosphate buffered 4% paraformaldehyde, cryoprotected with 20% sucrose, and embedded in optical cutting temperature (OCT) medium (Sakura Finetek USA, Torrance, CA). Immunohistochemistry (IHC) was performed as previously described (Taylor et al., 2015). 10-µm-thick sections, collected through the optic nerve head, were mounted on glass slides. Sections were washed in phosphate buffer saline with 0.5% Triton-x (PBST) and incubated in 20% heat-inactivated normal sheep serum for 2 hours (NSS; Sigma-Aldrich Corp., St Louis MO). Primary antibodies were applied overnight at 4°C. Sections were then washed with PBST and incubated in secondary antibodies for 1 hour at room temperature. Prior to IHC for BrdU, sections were immersed in 100°C sodium citrate buffer (10 mM sodium citrate, 0.05% Tween 20, pH 6.0) for 30 minutes and then cooled at room temperature for 20 minutes. Sections were then subjected to IHC as described above. IHC performed on whole retinas was conducted as described previously (Nagashima et al., 2017). Prior to IHC, retinas were dissected from dark-adapted animals, flattened with radial relaxing cuts, fixed at 4^0C overnight in 4% paraformaldehyde in 0.1M phosphate buffer with 5% sucrose. Wholemount retinas were isolated and immunostained following the protocol described in Nagashima et al. (2017). Antibodies used in this study and their concentrations are listed in Table 2.

Labeling dividing cells

Dividing cells were labeled with BrdU by housing animals in system water containing 5 mM BrdU for 24 hours (Gramage et al., 2015).

***In situ* Hybridization**

In situ hybridizations were performed as previously described (Luo et al., 2012). Digoxigenin (DIG)-labeled riboprobes for *rhodopsin* and *pde6c* were generated from full-length cDNA clones

(Luo et al., 2012; Ochocinska and Hitchcock, 2007), whereas riboprobe for *mmp-9* was generated by PCR amplification using primers containing the T3 or T7 promoter sequences (David and Wedlich, 2001). *mmp-9* (F): 5' TAATACGACTCACTATAGGGGATTCTTCTACTTCTGCCGGG 3' *mmp-9* (R): 5' AATTAACCCTCACTAAAGGGCTTAATAAATTTGTAAACAAG 3'.

Briefly, 10-µm-thick sections were hybridized with riboprobes at 55°C, incubated with an alkaline-phosphatase-conjugated anti-DIG antibody and visualized using Fast Red TR/Naphthol AS-MX (SIGMA*FAST*) as the enzymatic substrate. When *in situ* hybridizations were combined with BrdU IHC, sections were removed from the fast red solutions, rinsed and post-fixed in buffered 4% paraformaldehyde for 10 minutes then processed for BrdU IHC as described above.

Mmp-9 antibodies

Antibodies specific to zebrafish Mmp-9 were generated by Pocono Rabbit Farm & Laboratory (PRF&L, Canadensis, PA) as previously described (Calinescu et al., 2009). A 24 amino acid peptide was used as the immunogen CDIDGIQYLYGPRTGPEPTAPQPR; NCBI: AY151254. Polyclonal antibodies were affinity purified and confirmed by ELISA (data not shown). Western blots performed with retinal proteins using pre and post-immune sera confirmed the post-immune serum detected a 76 kDa band, the predicted size of Mmp-9.

Western Blot Analysis

Protein samples were obtained from whole retinas homogenized in RIPA lysis buffer (ThermoFisher Scienific, Waltham, MA) containing protease and phosphatase inhibitor cocktail (5872S; Cell Signaling Technology, Danvers, MA, USA). Each sample contained six pooled retinas from three adult fish. Proteins were separated in a 12% Mini-PROTEAN TGX Precast gel (BioRad; Hercules, CA) and transferred to a polyvinylidene difluoride (PVDF) membrane (GenHunter Corp., Nashville, TN). To block non-specific staining, membranes were incubated in 5% nonfat dry milk in Tris buffered saline containing 0.3% Tween-20 (TBST) for 2 hours.

Membranes were incubated with the antibodies-containing solution overnight at 4°C. Blots were then washed in TBST and incubated with horseradish peroxidase-conjugated secondary IgG (1:1000) for 1 hour at room temperature. Antibody-bound protein was visualized using Pierce ECL Western blotting substrate (32106; ThermoFisher Scienific, Waltham, MA). To visualize loading controls, blots were also stained with antibodies against actin. Images were captured using the Azure C500 (Azure Biosystems). Densitometry of protein bands was performed using ImageJ software (https://imagej.nih.gov/ij/).

Zymography

Protein samples were prepared as described for the Western blot analyses. Proteins were separated on 10% Zymogram Plus (Gelatin) Protein Gels, (ThermoFisher Scientific; Waltham, MA). Following electrophoresis, proteins were renatured in 1X renaturing buffer (ThermoFisher Scientific; Cat# LC2670) for 30 mins at room temperature, then incubated in 1X developing buffer (ThermoFisher Scientific; Cat# LC2671) overnight at 37º. Gels were rinsed in deionized water and stained with SimplyBlue SafeStain (ThermoFisher Scientific; Cat# LC6060). Gels were imaged with long-wave ultraviolet light using the Azure C500 (Azure Biosystems; Dublin, CA). Active recombinant human MMP-9 (Calbiochem; PF140) was used as a positive control. Densitometry of the digested bands was performed using ImageJ software.

Purification and intraocular injection of TNF-α

To express the soluble form of zebrafish Tnf-α, the pQE30 plasmid containing zebrafish Tnf-α cDNA was transfected into M15 cells (QIAGEN, Germantown, MD) as described previously (Nelson et al., 2014). IPTG (final concentration: 1 mM, isopropylthio-β-galactoside, Life Technologies; Carlsbad, CA) was used to induce Tnf-α protein expression. An empty vector, lacking the *tnf-α* cDNA, was used as the control. Control and Tnf-α samples were subjected to the same purification methods. Purified Tnf-α was diluted to 1 mg/ml. 0.5 µl of either control lysate or recombinant Tnf-α was intravitreally injected using a Hamilton syringe. Intravitreal

injections were repeated every 24 hours, and total RNA was collected at 72 hours post injection (hpi).

CRISPR-mediated gene mutation

mmp-9 mutants were generated according to previously described methods (Hwang et al., 2013). ZiFiT software (available in the public domain at zifit.partners.org) was used to identify the 19bp sgRNA target sequence for *mmp-9* (GGCTGCTTCATGGCATCAA). Target sequence Oligo1-TAGGCTGCTTCATGGCATCAA and Oligo2-AAACTTGATGCCATGAAGCAG were annealed and subcloned into the pT7 gRNA vector (Addgene ID: 46759). The pCS2 nCas9n vector (Addgene ID: 46929) was used for Cas9 synthesis. To produce RNAs, the MEGAshortscript T7 kit (Ambion: AM1354) and mirVana miRNA Isolation kit (Ambion: AM 1560) were used for the gRNA, whereas, mMesage mMACHINE SP6 kit (Ambion: AM1340) and RNeasy mini Kit from (Qiagen: 74104) were used for the Cas9 mRNA. Single cell-stage embryos were injected with a 2nL solution containing 100 pg/nl sgRNA and 150 pg/nl Cas9 mRNA. Founders (F0) were outcrossed to AB wild-type fish. Mutations were identified using screening primers (F: 5′- AAGTCTGCAACTACATATCAGC -3′, R: 5′-GTACACACTGTAGATGCTGATAAG-3') that flanked the *mmp-9* sgRNA target site. Standard protocols for PCR used Platinum Taq-HF polymerase (Invitrogen; Carlsbad, CA) with genomic DNA as the template. The purified PCR product was subcloned into the pGEM-T Easy vector (Promega, Madison, WI) for Sanger sequencing. Mutant and wild-type sequences were aligned using pairwise blast (National Center for Biotechnology Information [NCBI], Bethesda, MD, USA). Premature stop codons were identified by comparing predicted amino acid sequences for wild-type and mutants using the ExPASy translate tool (available in the public domain at (www.expasy.org). F1 hybrids carrying a *mmp-9* mutation were in-crossed and homozygous F2 mutants were identified by a combination of Sanger sequencing and T7 endonuclease assays (New England Biolabs, Ipswich, MA) as previously described (www.crisprflydesign.org).

Imaging and Statistical Analysis

Fluorescence images of retinal sections were captured using the Leica TCS SP5 confocal microscope (Wetzlar, Germany). Cell counts were conducted using z-stack images and analyzed with Imaris software (Bitplane, South Windsor, CT). Regenerated photoreceptors were identified by the colocalization of DAPI, BrdU, and the ISH markers *pde6c* (cones) or *rho* (rods). In wholemount retinas cone photoreceptors were counted from max projection images of control and mutant whole-mount retinas. For each retina, five separate regions, totaling 5625^2µm/retina, were sampled. Statistical comparisons between control and mutant retinas were performed using a Student's t-test by GraphPad Prism 5 (La Jolla, CA). ANOVA was performed using JMP 9.0 (SAS Institute, Inc; Cary, NC). A p-value less than 0.05 was considered a statistically significant difference.

Acknowledgements:
This work was supported by grants from the National Institutes of Health - R01 EY024519 (DRH), R01EY07060 (PFH), T32EY013934 (NJS), P30EYO7003 (PFH) and an unrestricted grant from the Research to Prevent Blindness, New York. The authors thank Dilip Pawar for technical assistance. Fish lines and reagents provided by ZIRC were supported by NIH-NCRR Grant P40 RR01.

The authors declare they have no competing financial or non-financial interests.

References

Amor S, Puentes F, Baker D, van der Valk P. 2010. Inflammation in neurodegenerative diseases. *Immunology* 129:154–169.

Ando K, Shibata E, Hans S, Brand M, Kawakami A. 2017. Osteoblast Production by Reserved Progenitor Cells in Zebrafish Bone Regeneration and Maintenance. *Dev Cell* 43:643–650.e3.

Bernardos RL, Barthel LK, Meyers JR, Raymond PA. 2007. Late-stage neuronal progenitors in the retina are radial Müller glia that function as retinal stem cells. *J Neurosci* 27:7028–7040.

Bernardos RL, Raymond PA. 2006. GFAP transgenic zebrafish. *Gene Expr Patterns* 6:1007–1013.

Bonnans C, Chou J, Werb Z. 2014. Remodelling the extracellular matrix in development and disease. *Nat Rev Mol Cell Biol* 15:786–801.

Borsini A, Zunszain PA, Thuret S, Pariante CM. 2015. The role of inflammatory cytokines as key modulators of neurogenesis. *Trends Neurosci* 38:145–157.

Bosak V, Murata K, Bludau O, Brand M. 2018. Role of the immune response in initiating central nervous system regeneration in vertebrates: learning from the fish. *Int J Dev Biol* 62:403–417.

Bringmann A, Pannicke T, Grosche J, Francke M, Wiedemann P, Skatchkov SN, Osborne NN, Reichenbach A. 2006. Müller cells in the healthy and diseased retina. *Prog Retin Eye Res* 25:397–424.

Bringmann A, Iandiev I, Pannicke T, Wurm A, Hollborn M, Wiedemann P, Osborne NN, Reichenbach A. 2009. Cellular signaling and factors involved in Müller cell gliosis: neuroprotective and detrimental effects. *Prog Retin Eye Res* 28:423–451.

Calinescu A-A, Raymond PA, Hitchcock PF. 2009. Midkine expression is regulated by the circadian clock in the retina of the zebrafish. *Vis Neurosci* 26:495–501.

Chattopadhyay S, Shubayev VI. 2009. MMP-9 controls Schwann cell proliferation and phenotypic remodeling via IGF-1 and ErbB receptor-mediated activation of MEK/ERK pathway. *Glia* 57:1316–1325.

Chen M, Xu H. 2012. Inflammation in Age-Related Macular Degeneration – Implications for TherapyInflammatory Diseases - Immunopathology, Clinical and Pharmacological Bases.

de Oliveira S, Reyes-Aldasoro CC, Candel S, Renshaw SA, Mulero V, Calado A. 2013. Cxcl8 (IL-8) mediates neutrophil recruitment and behavior in the zebrafish inflammatory response. *J Immunol* 190:4349–4359.

Deverman BE, Patterson PH. 2009. Cytokines and CNS Development. *Neuron* 64:61–78.

Ekdahl CT, Kokaia Z, Lindvall O. 2009. Brain inflammation and adult neurogenesis: the dual role of microglia. *Neuroscience* 158:1021–1029.

Fausett BV, Goldman D. 2006. A role for alpha1 tubulin-expressing Müller glia in regeneration of the injured zebrafish retina. *J Neurosci* 26:6303–6313.

Fimbel SM, Montgomery JE, Burket CT, Hyde DR. 2007. Regeneration of inner retinal neurons after intravitreal injection of ouabain in zebrafish. J Neurosci. 14:1712-24.

Fischer AJ, Zelinka C, Gallina D, Scott MA, Todd L. 2014. Reactive microglia and macrophage facilitate the formation of Müller glia-derived retinal progenitors. *Glia* 62:1608–1628.

Fritsche LG, Igl W, Bailey JNC, Grassmann F, Sengupta S, Bragg-Gresham JL, Burdon KP, Hebbring SJ, Wen C, Gorski M, Kim IK, Cho D, Zack D, Souied E, Scholl HPN, Bala E, Lee KE, Hunter DJ, Sardell RJ, Mitchell P, Merriam JE, Cipriani V, Hoffman JD, Schick T, Lechanteur YTE, Guymer RH, Johnson MP, Jiang Y, Stanton CM, Buitendijk GHS, Zhan X, Kwong AM, Boleda A, Brooks M, Gieser L, Ratnapriya R, Branham KE, Foerster JR, Heckenlively JR, Othman MI, Vote BJ, Liang HH, Souzeau E, McAllister IL, Isaacs T, Hall J, Lake S, Mackey DA, Constable IJ, Craig JE, Kitchner TE, Yang Z, Su Z, Luo H, Chen D,

Ouyang H, Flagg K, Lin D, Mao G, Ferreyra H, Stark K, von Strachwitz CN, Wolf A, Brandl C, Rudolph G, Olden M, Morrison MA, Morgan DJ, Schu M, Ahn J, Silvestri G, Tsironi EE, Park KH, Farrer LA, Orlin A, Brucker A, Li M, Curcio CA, Mohand-Saïd S, Sahel J-A, Audo I, Benchaboune M, Cree AJ, Rennie CA, Goverdhan SV, Grunin M, Hagbi-Levi S, Campochiaro P, Katsanis N, Holz FG, Blond F, Blanché H, Deleuze J-F, Igo RP Jr, Truitt B, Peachey NS, Meuer SM, Myers CE, Moore EL, Klein R, Hauser MA, Postel EA, Courtenay MD, Schwartz SG, Kovach JL, Scott WK, Liew G, Tan AG, Gopinath B, Merriam JC, Smith RT, Khan JC, Shahid H, Moore AT, McGrath JA, Laux R, Brantley MA Jr, Agarwal A, Ersoy L, Caramoy A, Langmann T, Saksens NTM, de Jong EK, Hoyng CB, Cain MS, Richardson AJ, Martin TM, Blangero J, Weeks DE, Dhillon B, van Duijn CM, Doheny KF, Romm J, Klaver CCW, Hayward C, Gorin MB, Klein ML, Baird PN, den Hollander AI, Fauser S, Yates JRW, Allikmets R, Wang JJ, Schaumberg DA, Klein BEK, Hagstrom SA, Chowers I, Lotery AJ, Léveillard T, Zhang K, Brilliant MH, Hewitt AW, Swaroop A, Chew EY, Pericak-Vance MA, DeAngelis M, Stambolian D, Haines JL, Iyengar SK, Weber BHF, Abecasis GR, Heid IM. 2016. A large genome-wide association study of age-related macular degeneration highlights contributions of rare and common variants. *Nat Genet* 48:134–143.

Gemberling M, Bailey TJ, Hyde DR, Poss KD. 2013. The zebrafish as a model for complex tissue regeneration. *Trends Genet* 29:611–620.

Goldman D. 2014. Müller glial cell reprogramming and retina regeneration. *Nat Rev Neurosci* 15:431–442.

Gorsuch RA, Hyde DR. 2014. Regulation of Müller glial dependent neuronal regeneration in the damaged adult zebrafish retina. *Exp Eye Res* 123:131–140.

Gramage E, D'Cruz T, Taylor S, Thummel R, Hitchcock PF. 2015. Midkine-a Protein Localization in the Developing and Adult Retina of the Zebrafish and Its Function During Photoreceptor Regeneration. *PLoS One* 10:e0121789.

Hindi SM, Shin J, Ogura Y, Li H, Kumar A. 2013. Matrix Metalloproteinase-9 Inhibition Improves Proliferation and Engraftment of Myogenic Cells in Dystrophic Muscle of mdx Mice. *PLoS One* 8:e72121.

Hwang WY, Fu Y, Reyon D, Maeder ML, Tsai SQ, Sander JD, Peterson RT, Yeh J-RJ, Keith Joung J. 2013. Efficient genome editing in zebrafish using a CRISPR-Cas system. *Nat Biotechnol* 31:227–229.

Karra R, Knecht AK, Kikuchi K, Poss KD. 2015. Myocardial NF-κB activation is essential for zebrafish heart regeneration. *Proc Natl Acad Sci U S A* 112:13255–13260.

Kauppinen A, Paterno JJ, Blasiak J, Salminen A, Kaarniranta K. 2016. Inflammation and its role in age-related macular degeneration. *Cell Mol Life Sci* 73:1765–1786.

Kaur S, Gupta S, Chaudhary M, Khursheed MA, Mitra S, Kurup AJ, Ramachandran R. 2018. let-7 MicroRNA-Mediated Regulation of Shh Signaling and the Gene Regulatory Network Is Essential for Retina Regeneration. *Cell Rep* 23:1409–1423.

Kizil C, Kaslin J, Kroehne V, Brand M. 2012. Adult neurogenesis and brain regeneration in zebrafish. *Dev Neurobiol* 72:429–461.

Kizil C, Kyritsis N, Brand M. 2015. Effects of inflammation on stem cells: together they strive? *EMBO Rep* 16:416–426.

Kok FO, Shin M, Ni CW, Gupta A, Grosse AS, van Impel A, Kirchmaier BC, Peterson-Maduro J, Kourkoulis G, Male I, DeSantis DF, Sheppard-Tindell S, Ebarasi L, Betsholtz C, Schulte-Merker S, Wolfe SA, Lawson ND 2015. Reverse genetic screening revealspoor correlation between morpholino-induced and mutant phenotypes in zebrafish. Dev Cell 32:97–108.

Kyritsis N, Kizil C, Brand M. 2014. Neuroinflammation and central nervous system regeneration in vertebrates. *Trends Cell Biol* 24:128–135.

Kyritsis N, Kizil C, Zocher S, Kroehne V, Kaslin J, Freudenreich D, Iltzsche A, Brand M. 2012. Acute inflammation initiates the regenerative response in the adult zebrafish brain. *Science* 338:1353–1356.

Lagman D, Callado-Pérez A, Franzén IE, Larhammar D, Abalo XM. 2015. Transducin duplicates in the zebrafish **retina** and pineal complex: differential specialisation after the teleost tetraploidisation. PLoS One. 10(3):e0121330. doi: 10.1371/journal.pone.0121330.

LeBert DC, Squirrell JM, Rindy J, Broadbridge E, Lui Y, Zakrzewska A, Eliceiri KW, Meijer AH, Huttenlocher A. 2015. Matrix metalloproteinase 9 modulates collagen matrices and wound repair. *Development* 142:2136–2146.

Lenkowski JR, Raymond PA. 2014. Müller glia: Stem cells for generation and regeneration of retinal neurons in teleost fish. *Prog Retin Eye Res* 40:94–123.

Le NTV, Xue M, Castelnoble LA, Jackson CJ. 2007. The dual personalities of matrix metalloproteinases in inflammation. *Front Biosci* 12:1475–1487.

Liddiard K, Rosas M, Davies LC, Jones SA, Taylor PR. 2011. Macrophage heterogeneity and acute inflammation. *Eur J Immunol* 41:2503–2508.

Luo J, Uribe RA, Hayton S, Calinescu A-A, Gross JM, Hitchcock PF. 2012. Midkine-A functions upstream of Id2a to regulate cell cycle kinetics in the developing vertebrate retina. *Neural Dev* 7:33.

Manicone A, Mcguire J. 2008. Matrix metalloproteinases as modulators of inflammation. *Semin Cell Dev Biol* 19:34–41.

Masure S, Proost P, Van Damme J, Opdenakker G. 1991. Purification and identification of 91-kDa neutrophil gelatinase. Release by the activating peptide interleukin-8. *Eur J Biochem* 198:391–398.

Nagashima M, Barthel LK, Raymond PA. 2013. A self-renewing division of zebrafish Müller glial cells generates neuronal progenitors that require N-cadherin to regenerate retinal neurons. *Development* 140:4510–4521.

Nagashima M, Hadidjojo J, Barthel LK, Lubensky DK, Raymond PA. 2017. Anisotropic Müller glial scaffolding supports a multiplex lattice mosaic of photoreceptors in zebrafish retina. *Neural Dev* 12:20.

Nathan C. 2002. Points of control in inflammation. *Nature* 420:846–852.

Nelson CM, Gorsuch RA, Bailey TJ, Ackerman KM, Kassen SC, Hyde DR. 2012. Stat3 defines three populations of Müller glia and is required for initiating maximal müller glia proliferation in the regenerating zebrafish retina. *J Comp Neurol* 520:4294–4311.

Nelson CM, Ackerman KM, O'Hayer P, Bailey TJ, Gorsuch RA, Hyde DR. 2013. Tumor necrosis factor-alpha is produced by dying retinal neurons and is required for Muller glia proliferation during zebrafish retinal regeneration. *J Neurosci* 33:6524–6539.

Ochocinska MJ, Hitchcock PF. 2007. Dynamic expression of the basic helix-loop-helix transcription factor neuroD in the rod and cone photoreceptor lineages in the retina of the embryonic and larval zebrafish. *J Comp Neurol* 501:1–12.

Parks WC, Wilson CL, López-Boado YS. 2004. Matrix metalloproteinases as modulators of inflammation and innate immunity. *Nat Rev Immunol* 4:617–629.

Powell C, Cornblath E, Elsaeidi F, Wan J, Goldman D. 2016. Zebrafish Müller glia-derived progenitors are multipotent, exhibit proliferative biases and regenerate excess neurons. *Sci Rep* 6:24851.

Ramachandran R, Zhao X-F, Goldman D. 2012. Insm1a-mediated gene repression is essential for the formation and differentiation of Müller glia-derived progenitors in the injured retina. *Nat Cell Biol* 14:1013–1023.

Raymond PA, Barthel LK, Bernardos RL, Perkowski JJ. 2006. Molecular characterization of retinal stem cells and their niches in adult zebrafish. *BMC Dev Biol* 6:36.

Reichenbach A, Bringmann A. 2013. New functions of Müller cells. *Glia* 61:651–678.

Roesch K, Stadler MB, Cepko CL. 2012. Gene expression changes within Müller glial cells in retinitis pigmentosa. *Mol Vis* 18:1197–1214.

Schulte-Merker S, Stainier DYR. 2014. Out with the old, in with the new: Reassessing morpholino knockdowns in light of genome editing technology. Development 141:3103–

3104.
Sherpa T, Fimbel SM, Mallory DE, Maaswinkel H, Spritzer SD, Sand JA, Li L, Hyde DR, Stenkamp DL. 2008. Ganglion cell regeneration following whole-retina destruction in zebrafish. Dev Neurobiol. 68:166-81.
Shubayev VI, Angert M, Dolkas J, Marie Campana W, Palenscar K, Myers RR. 2006. TNFα-induced MMP-9 promotes macrophage recruitment into injured peripheral nerve. *Mol Cell Neurosci* 31:407–415.
Sifuentes CJ, Kim J-W, Swaroop A, Raymond PA. 2016. Rapid, Dynamic Activation of Müller Glial Stem Cell Responses in Zebrafish. *Invest Ophthalmol Vis Sci* 57:5148–5160.
Stenkamp DL. 2011. The rod photoreceptor lineage of teleost fish. *Prog Retin Eye Res* 30:395–404.
Stainier DYR, Raz E, Lawson ND, Ekker SC, Burdine RD, Eisen JS, Ingham PW, Schulte-Merker S, Yelon D, Weinstein BM, Mullins MC, Wilson SW, Ramakrishnan L, Amacher SL, Neuhauss SCF, Meng A, Mochizuki N, Panula P, Moens CB. 2017. Guidelines for morpholino use in zebrafish. PLoS Genet. 13(10):e1007000. doi: 10.1371
Taylor SM, Alvarez-Delfin K, Saade CJ, Thomas JL, Thummel R, Fadool JM, Hitchcock PF. 2015. The bHLH Transcription Factor NeuroD Governs Photoreceptor Genesis and Regeneration Through Delta-Notch Signaling. *Invest Ophthalmol Vis Sci* 56:7496–7515.
Ueki Y, Wilken MS, Cox, KE, Chipman L, Jorstad N, Sternhagen K, Simic M, Ullom K, Nakafuku M, Reh TA. 2015. Transgenic expression of the proneural transcription factor Ascl1 in Müller glia stimulates retinal regeneration in young mice. *Proc Nat Acad Sci* 112:13737-13722.
Vandooren J, Geurts N, Martens E, Van den Steen PE, Opdenakker G. 2013a. Zymography methods for visualizing hydrolytic enzymes. *Nat Methods* 10:211–220.
Vandooren J, Van den Steen PE, Opdenakker G. 2013b. Biochemistry and molecular biology of gelatinase B or matrix metalloproteinase-9 (MMP-9): the next decade. *Crit Rev Biochem Mol Biol* 48:222–272.
Vandooren J, Van Damme J, Opdenakker G. 2014. On the structure and functions of gelatinase B/matrix metalloproteinase-9 in neuroinflammation. *Prog Brain Res* 214:193–206.
Vecil GG, Larsen PH, Corley SM, Herx LM, Besson A, Goodyer CG, Yong VW. 2000. Interleukin-1 is a key regulator of matrix metalloproteinase-9 expression in human neurons in culture and following mouse brain trauma in vivo. *J Neurosci Res* 61:212–224.
Vetter ML, Hitchcock PF, and the AGI workshop participants Report on the National Eye Institute Audacious Goals Initiative: Replacement of Retinal Ganglion Cells from Endogenous Cell Sources. Transl Vis Sci Technol. 2017 Mar 15;6(2):5.
Walsh CE, Hitchcock PF. 2017. Progranulin regulates neurogenesis in the developing vertebrate retina. *Dev Neurobiol* 77:1114–1129.
Wan J, Ramachandran R, Goldman D. 2012. HB-EGF is necessary and sufficient for Müller glia dedifferentiation and retina regeneration. *Dev Cell* 22:334–347.
Whitcup SM, Nussenblatt RB, Lightman SL, Hollander DA. 2013. Inflammation in Retinal Disease. *Int J Inflam* 2013:1–4.
White DT, Sengupta S, Saxena MT, Xu Q, Hanes J, Ding D, Ji H, Mumm JS. 2017. Immunomodulation-accelerated neuronal regeneration following selective rod photoreceptor cell ablation in the zebrafish retina. *Proceedings of the National Academy of Sciences* 114:E3719–E3728.
Xue Q, Cao L, Chen X-Y, Zhao J, Gao L, Li S-Z, Fei Z. 2017. High expression of MMP9 in glioma affects cell proliferation and is associated with patient survival rates. *Oncol Lett* 13:1325–1330.
Xu S, Webb SE, Lau TCK, Cheng SH. 2018. Matrix metalloproteinases (MMPs) mediate leukocyte recruitment during the inflammatory phase of zebrafish heart regeneration. *Sci Rep* 8:7199.

Yoshida N, Ikeda Y, Notomi S, Ishikawa K, Murakami Y, Hisatomi T, Enaida H, Ishibashi T. 2013. Laboratory evidence of sustained chronic inflammatory reaction in retinitis pigmentosa. *Ophthalmology* 120:e5–12.

Zhao X-F, Wan J, Powell C, Ramachandran R, Myers MG, Goldman D. 2014. Leptin and IL-6 Family Cytokines Synergize to Stimulate Müller Glia Reprogramming and Retina Regeneration. *Cell Rep* 9:272–284.

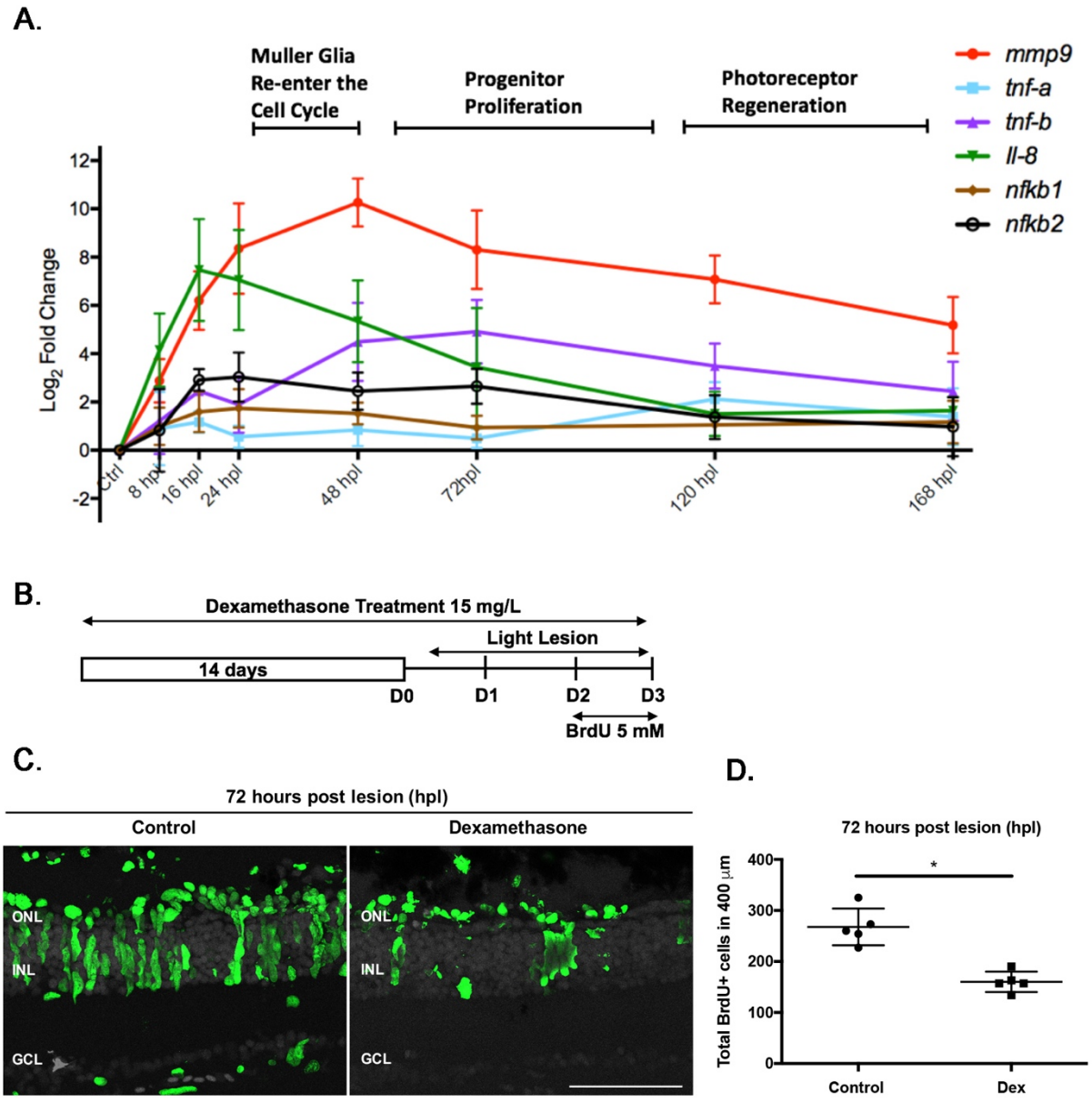

Figure 1: Inflammation is induced following photoreceptor death and regulates reactive-proliferation.
(A) Time-course for the expression of inflammatory genes, from 8 to 168 hours post lesion (hpl). Unlesioned retinas served as controls. Expression levels are represented as fold change calculated using DDC_T method. **(B)** Experimental paradigm for anti-inflammatory treatment with Dex and BrdU labeling. **(C)** BrdU immunostained cells (green) in controls (left) and Dex-treated animals (right) at 72 hpl. **(D)** Number of BrdU-labeled cells in controls (268 ± 36.1 cells) and Dex-treated animals (160.2 ± 20.02 cells) at 72 hpl; *p=0.0079. ONL- outer nuclear layer; INL- inner nuclear layer; GCL- ganglion cell layer. Scale bar equals 50μm.

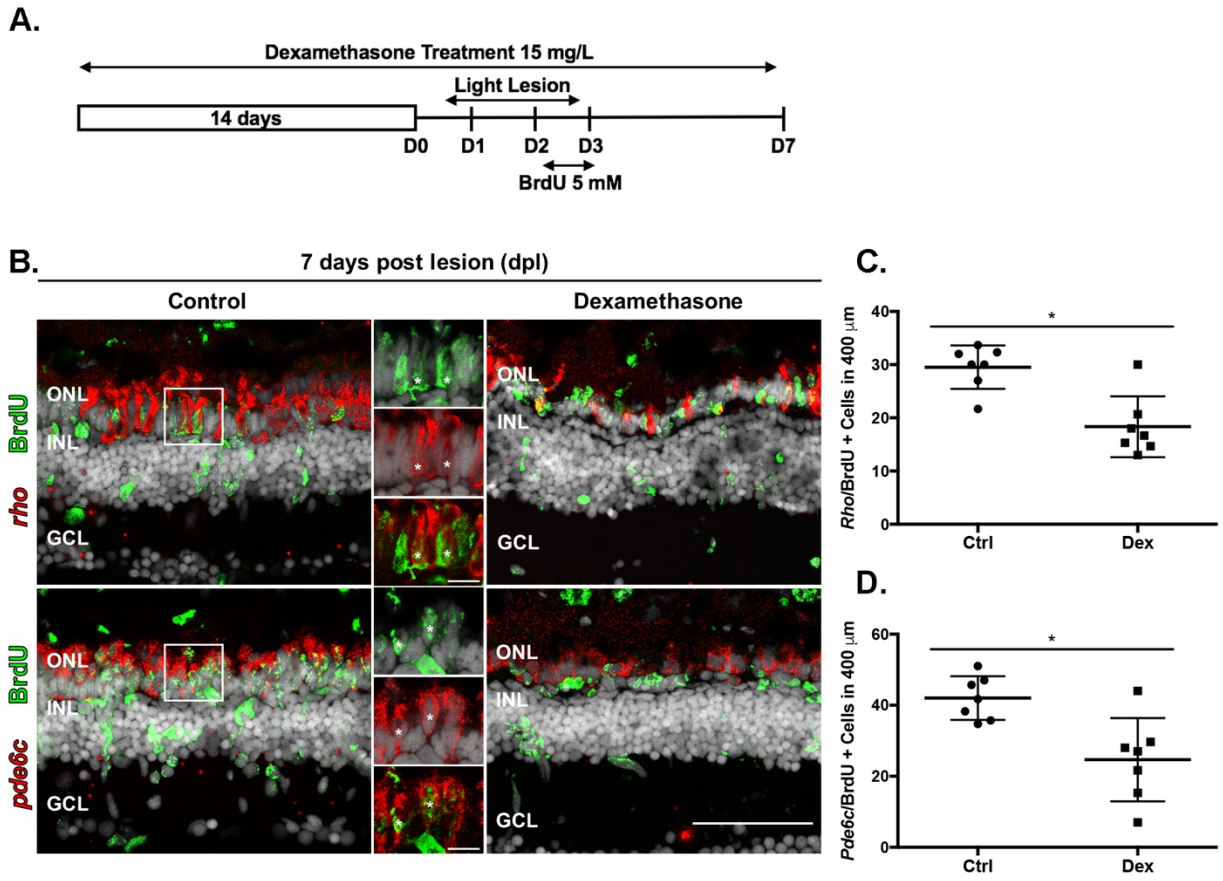

Figure 2: Anti-inflammatory treatment suppresses photoreceptor regeneration. **(A)** Experimental paradigm of anti-inflammatory treatment. **(B)** Double labeled, regenerated photoreceptors using *in situ* hybridization for rods (*rho) and cones (pde6c;* red signal) and BrdU (green). The high magnification insets show the colocalization of the two labels. Control retinas are left; Dex-treated retinas are right. **(C)** Number of regenerated rod photoreceptors in control (42 ± 6.1 cells) and experimental retinas (25 ± 11.72 cells); *p=0.0047. **(D)** Number of regenerated cone photoreceptors in control (29.52 ± 4.1 cells) and Dex-treated animals (18.33 ± 5.71 cells). *p=0.0012. ONL- outer nuclear layer; INL- inner nuclear layer; GCL- ganglion cell layer. Scale bar equals 50μm.

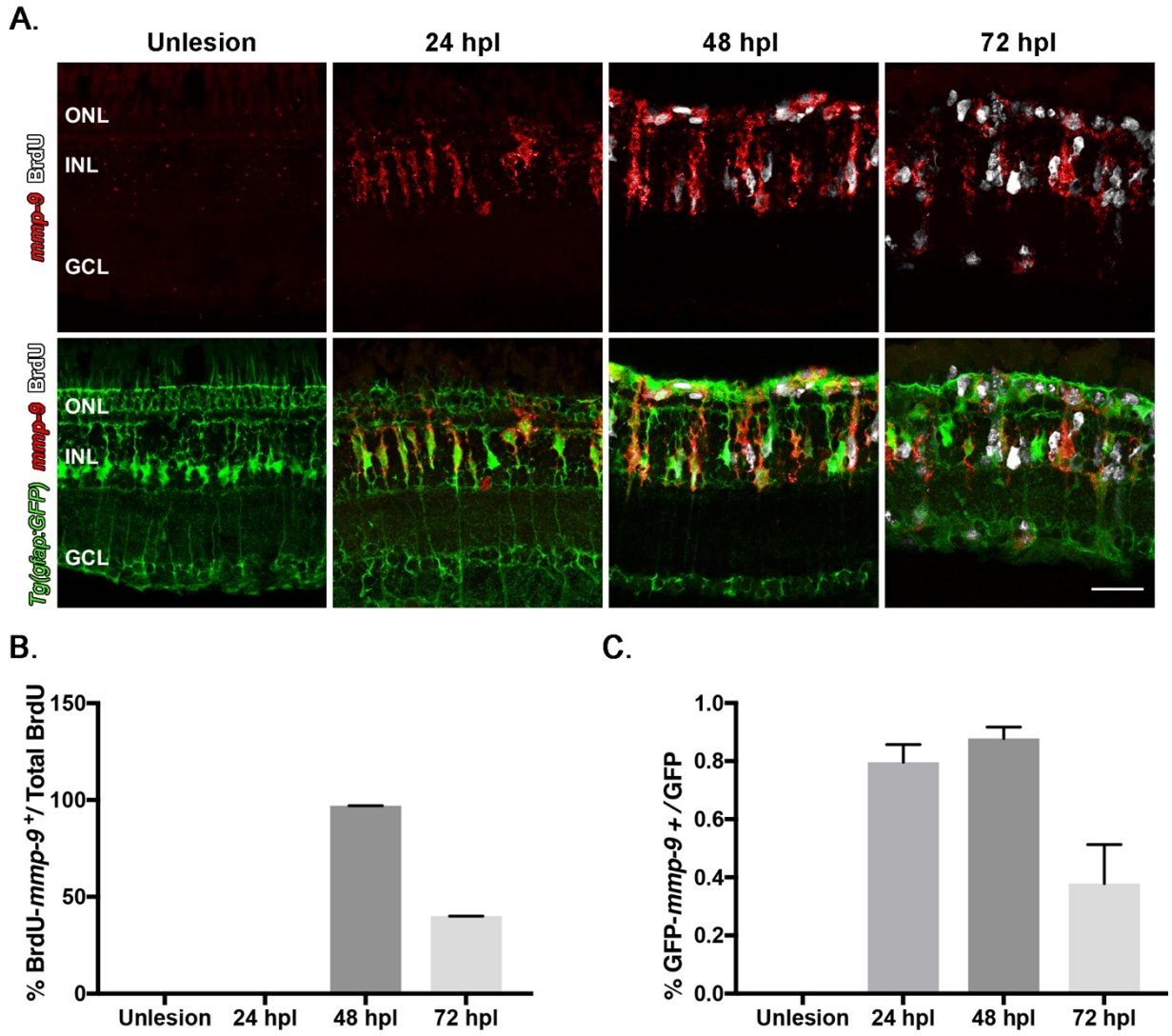

Figure 3: Following a photolytic lesion, Müller glia and Müller glia-derived progenitors express *mmp-9*.
These experiments were performed using the transgenic line *Tg[gfap:EGFP]mi2002*, in which eGFP is expressed in Müller glia. **(A)** Triple labeling using *in situ* hybridization for *mmp-9* (red signal) and immunostaining for BrdU for dividing cells (white; top row), combined with GFP immunostaining (green; bottom row). **(B)** Number of BrdU+ cells that express *mmp-9* in unlesioned animals and lesioned animals at 24, 48, and 72 hpl. **(C)** Number of GFP+ Müller glia that also express *mmp-9* expression at 24, 48, and 72 hpl. ONL- outer nuclear layer; INL- inner nuclear layer; GCL- ganglion cell layer. Scale bar equals 25μm.

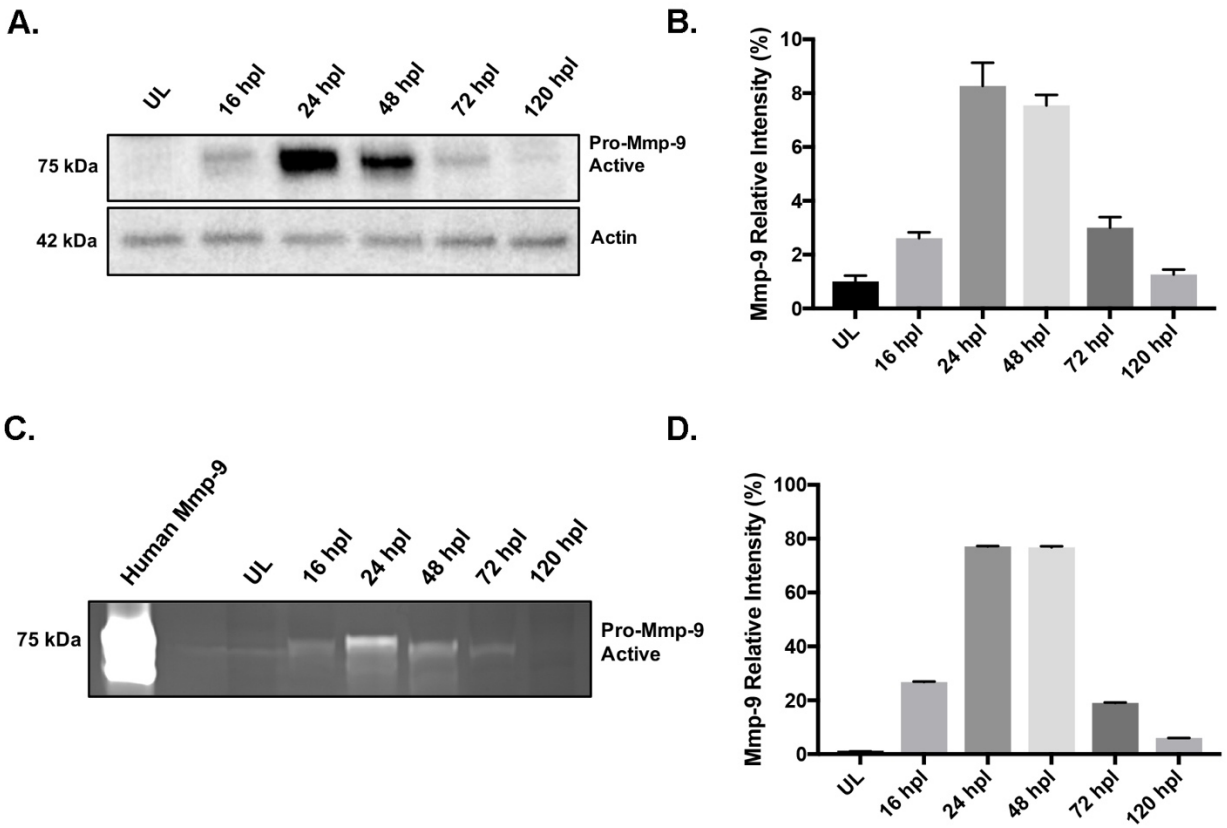

Figure 4: Mmp-9 is expressed and catalytically active following photoreceptor death.
(A) Western blot of retinal proteins from unlesioned retinas (UL) and lesioned retinas at 16 hpl, 24 hpl, 48 hpl, 72 hpl, and 120 hpl, stained with anti-Mmp-9 and anti-actin (loading control) antibodies. **(B)** Densitometry of Mmp-9 protein. **(C)** Zymogram of Mmp-9 catalytic activity from unlesioned retinas (UL) and lesioned retinas at 16, 24, 48, 72 and 120hpl. Lanes in zymogram correspond to those in the Western blot. Purified human recombinant protein serves as a positive control. **(D)** Densitometry of Mmp-9 catalytic activity.

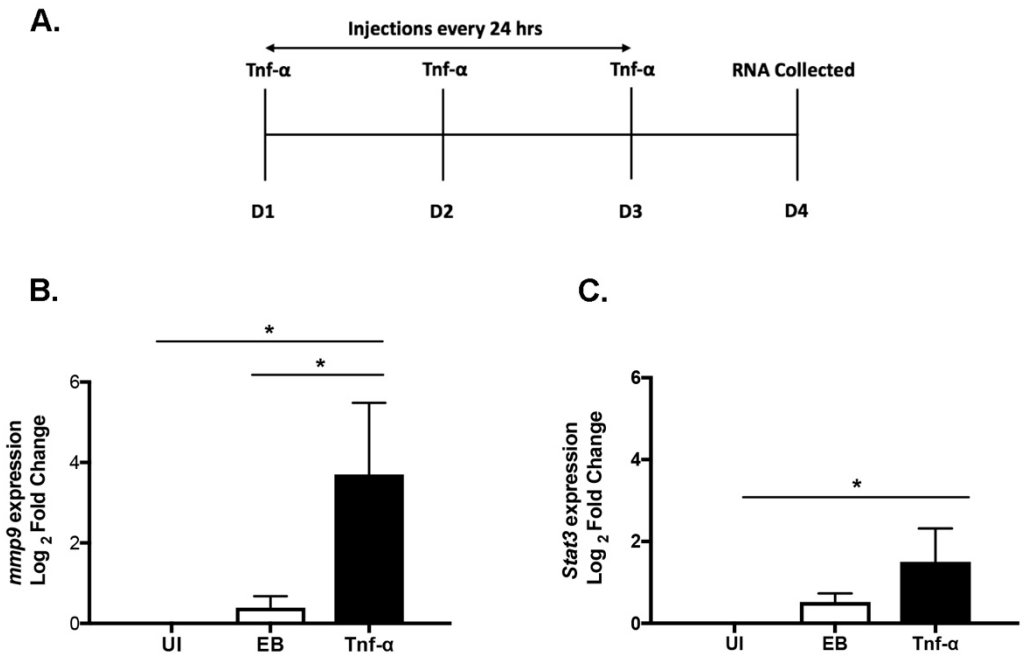

Figure 5: *mmp-9* is a component of the inflammatory response.
(A) Experimental paradigm for the intraocular injections of TNF-α into unlesioned retinas and mRNA collection. **(B)** qRT-PCR for *mmp-9* expression in uninjected retinas (UI), retinas exposed to elution buffer only (EB), and retinas exposed to TNF-α. *p=0.0229. **(C)** qRT-PCR for *stat3* gene expression in uninjected retinas (UI), retinas exposed to elution buffer only (EB), and retinas exposed to TNF-α. *p=0.0344.

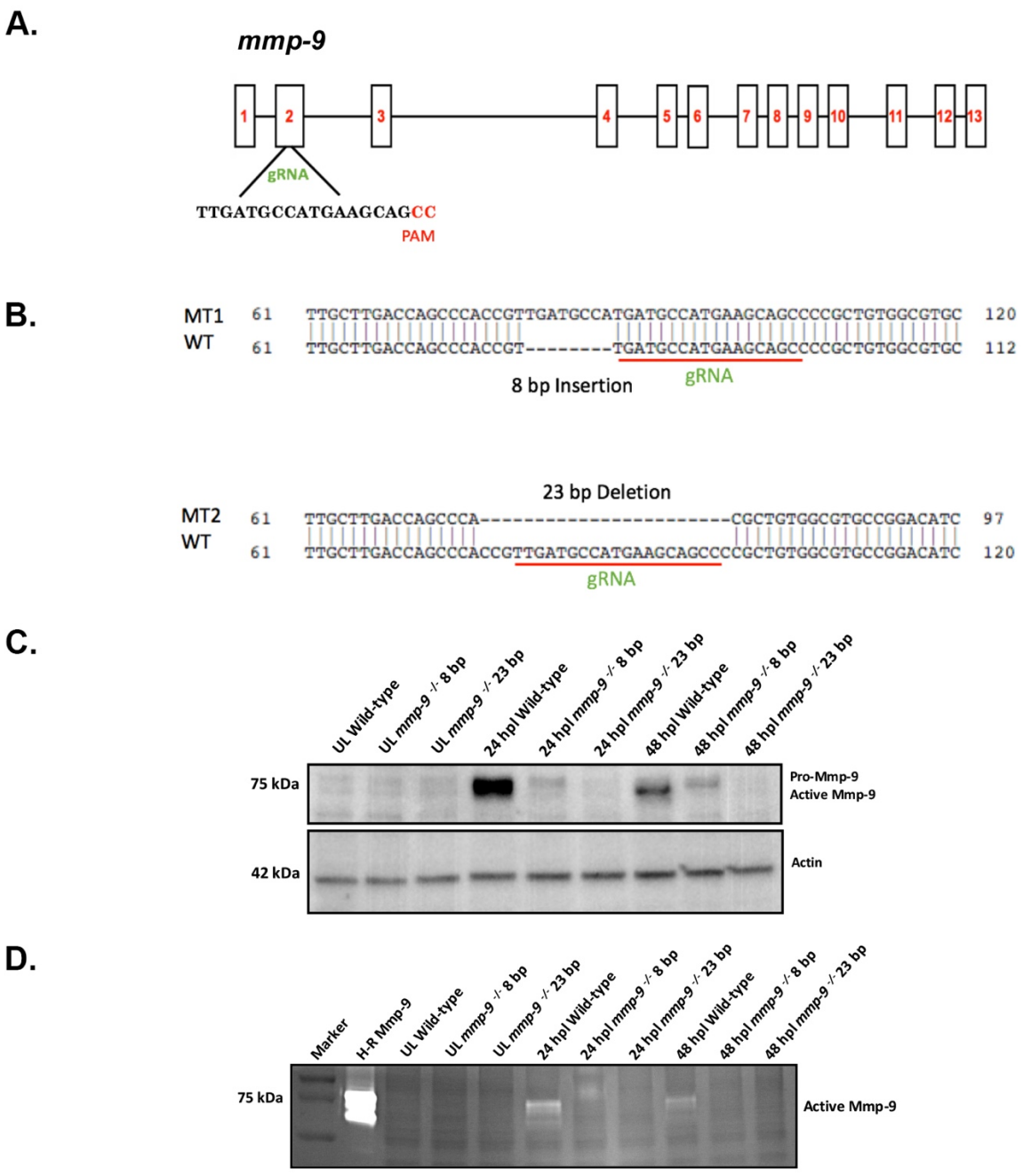

Figure 6: CRISPR mutants lack catalytically-active Mmp-9.
(A) Genomic structure of *mmp-9* and the gRNA target sequence. **(B)** Sequence alignment for two indel mutations - 8 bp insertion and 23 bp deletion. Red underline indicates the sequence targeted by the 19 bp gRNA. **(C)** Western blot of retinal proteins from unlesioned retinas (UL wild-type; UL *mmp-9*$^{-/-}$ 8bp; UL *mmp-9*$^{-/-}$ 23bp) and lesioned retinas (wild-type; *mmp-9*$^{-/-}$ 8bp; *mmp-9*$^{-/-}$ 23bp) at 16, 24, and 48hpl stained with anti-Mmp-9 and anti-actin (loading control) antibodies. **(D)** Zymogram of Mmp-9 catalytic activity. Lanes in zymogram correspond to those in the Western blot. Purified human recombinant protein serves as a positive control.

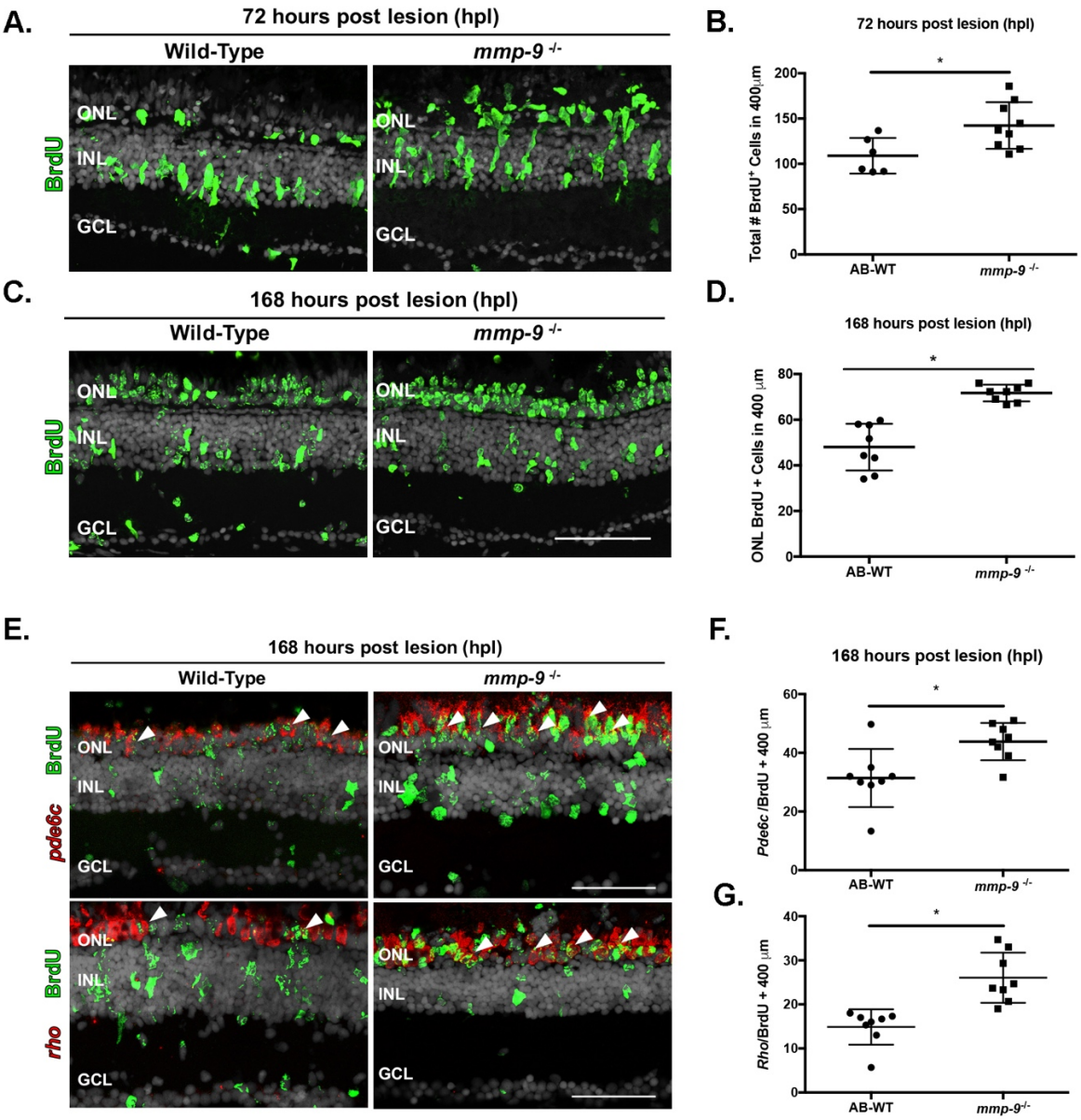

Figure 7: Photolytic lesions in *mmp-9* mutants results in the over production of injury-induced progenitors and regenerated photoreceptors.
(A) BrdU-labeled cells (green) in wild-type and *mmp-9* $^{-/-}$ mutants. **(B)** Number of BrdU+ cells from wild-type (109 ± 19.66 cells) mutant retinas (142.3 ± 25.72 cells) at 72 hpl. *p = 0.0186. **(C)** BrdU-labeled cells (green) in wild-type and mutant retinas at 168 hpl. **(D)** Number of BrdU+ cells in the ONL of wild-type (48 ± 10.24 cells) and mutant retinas (71.71 ± 3.7 cells). *p=0.0001. **(E)** Double labeled, regenerated photoreceptors using *in situ* hybridization for rods (*rho) and cones (pde6c;* red signal) and BrdU (green) at 168hpl. **(F)** Number of regenerated cone photoreceptors in wild-type (31.42 ± 9.88 cell) and mutant retinas (43.83 ± 10.68 cells) at 168 hpl. *p=0.0301. **(G)** Number of regenerated rod photoreceptors in wild-type (14.88 ± 4.02 cells) and mutant retinas (26.04 ± 5.69 cells) at 168 hpl. *p=0.0005. . ONL- outer nuclear layer; INL- inner nuclear layer; GCL- ganglion cell layer. Scale bars equal 50μm.

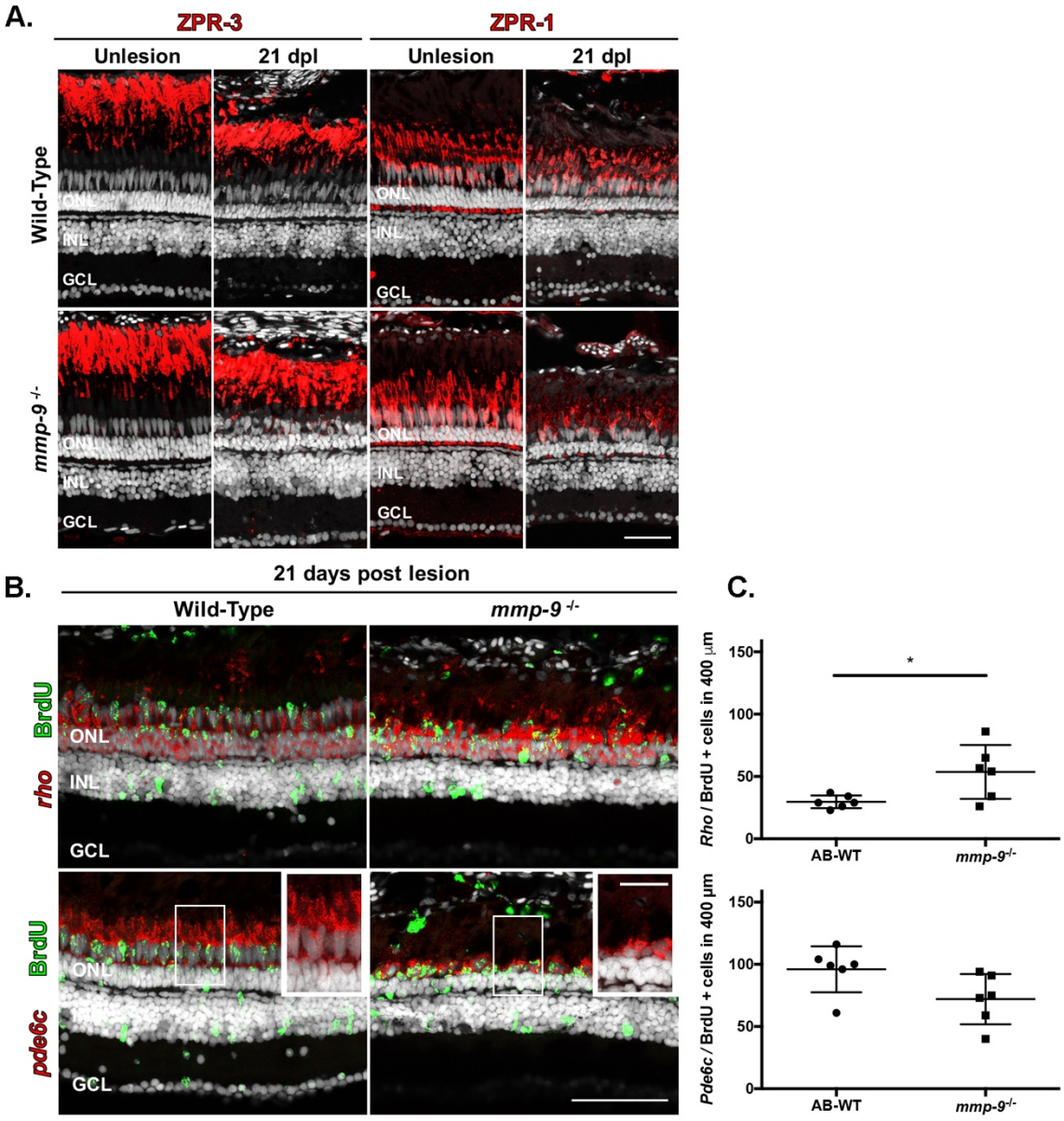

Fig 8. Mmp-9 regulates the maturation of regenerated photoreceptors.
(A) Immunostaining for red-green double cones with ZPR-1 and rods with ZPR-3. Wild-type are in the top row; mutants are in the bottom row. Unlesioned retinas are left; lesioned retinas at21 dpl are right. **(B)** Double labeled, regenerated photoreceptors at 21dpl using *in situ* hybridization for rods (*rho) and cones (pde6c;* red signal) and BrdU (green). Insets detail the morphology of regenerated photoreceptors in wild-type (left) and mutant retinas (right). **(C)** Number of regenerated cone photoreceptors (bottom) in wild-type (95.81 ± 18.49 cells) and mutant retinas (71.89 ± 20.37 cells) at 21 dpl. p=0.059. Number of of regenerated rod photoreceptors (top) in wild-type (29.6 ± 4.94 cells) and mutant retinas (53.39 ± 21.62 cells) at 21 dpl. *p=0.0270. ONL- outer nuclear layer; INL- inner nuclear layer; GCL- ganglion cell layer. Scale bar equals 50μm.

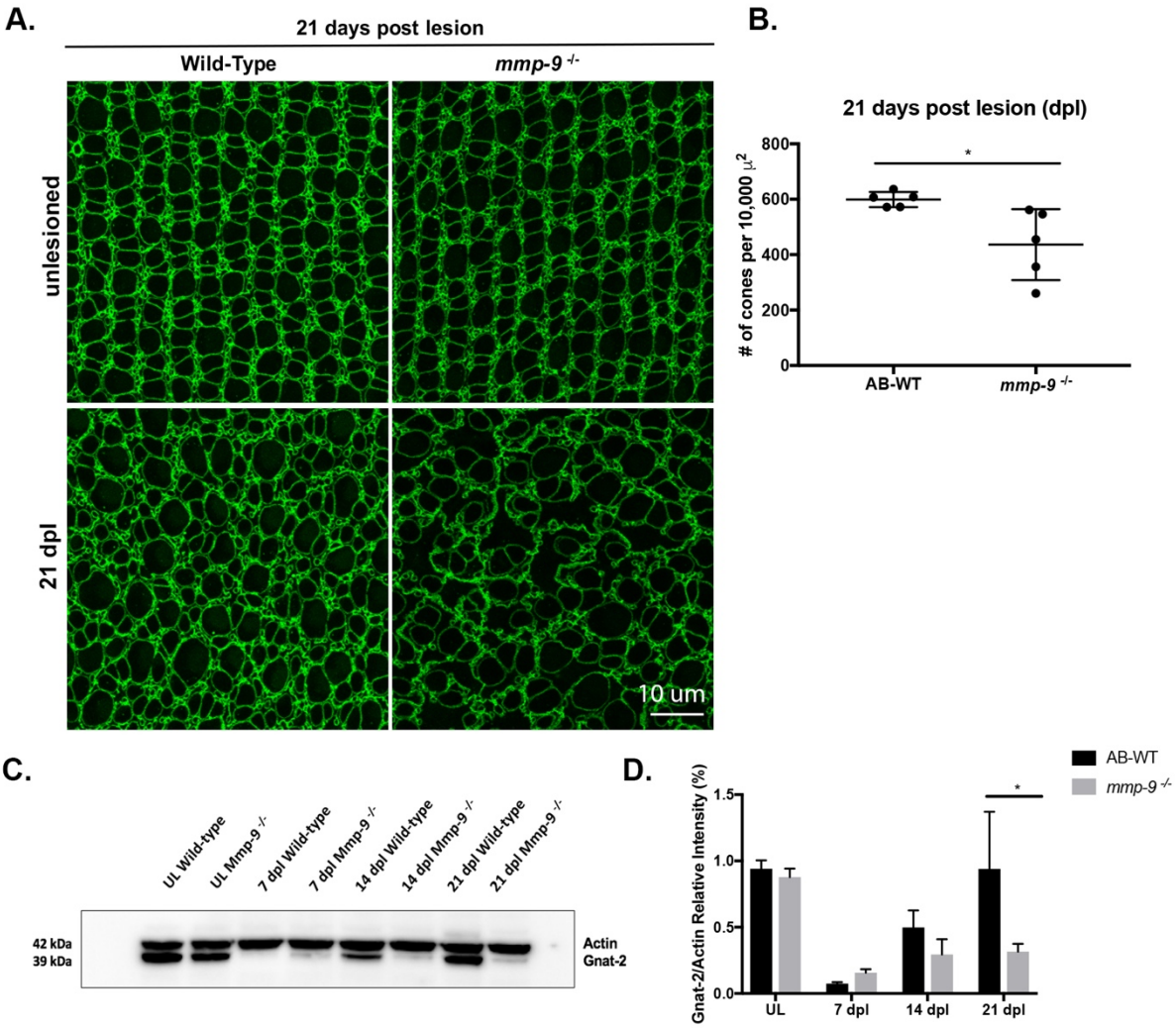

Fig 9. Mmp-9 is required for the survival of regenerated cone photoreceptors. **(A)** Wholemounts of wild-type (left) and mutant retinas (right) immunostained for ZO-1. Unlesioned retinas are top; lesioned retinas at 21dpl are bottom. **(B)** Number of regenerated cones from wild-type (599.11 ± 27.42 cones) and mutant retinas (436.09 ± 128.04 cones). *p=0.0238. **(C)** Western blot of retinas stained with antibodies against gnat-2 and actin at 7, 14, and 21 dpl. **(D)** Densitometry of gnat-2 labeling in the Western blot. A significant difference in gnat-2 levels were observed at 21 dpl. *p=.0014. Scale bar equals 10 μm.

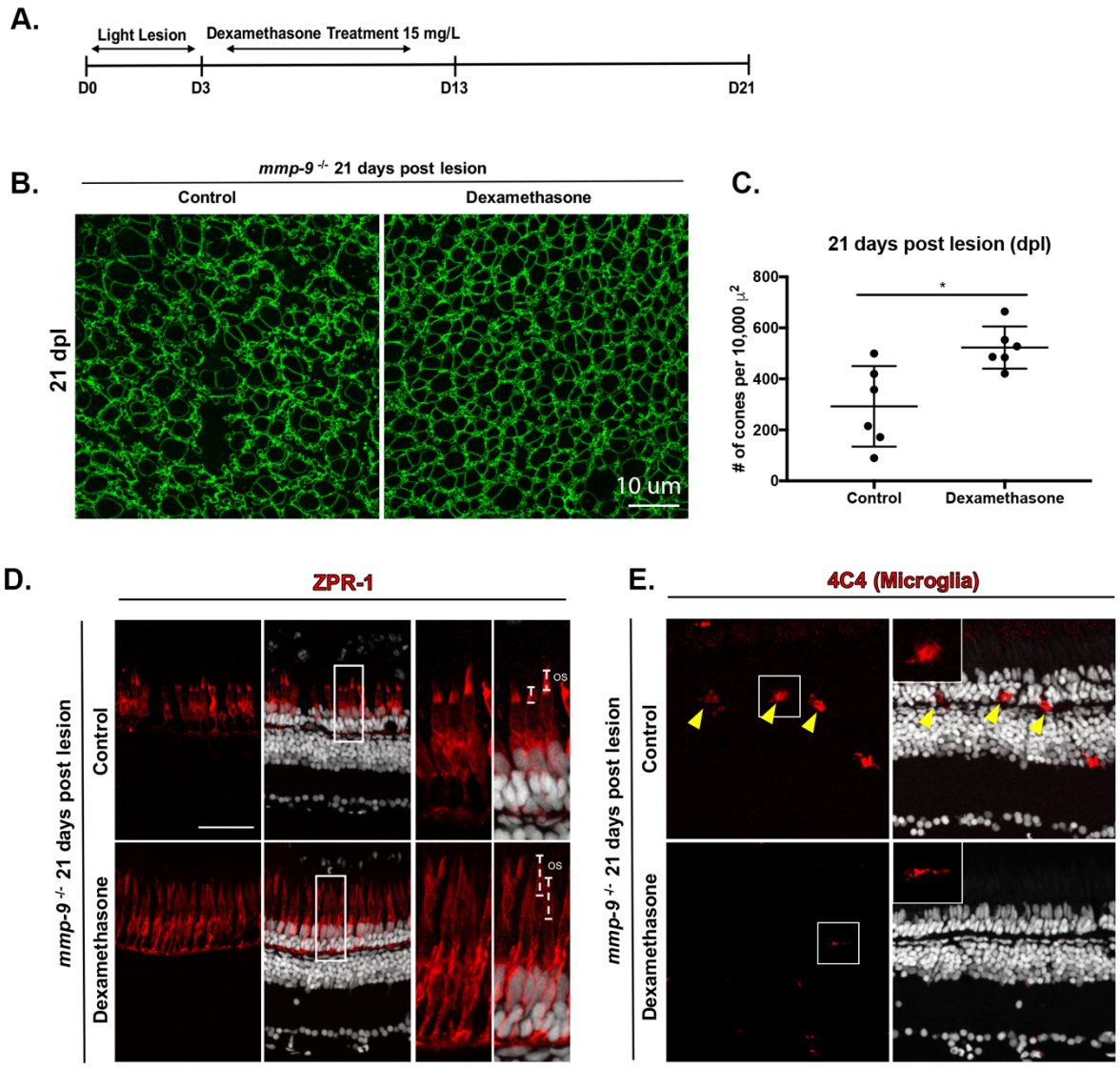

Fig 10. Anti-inflammatory treatment rescues the maturation and number of regenerated cones in mutants at 21dpl.
(A) Experimental paradigm for the photolytic lesions and Dexamethasone treatment used at 21 dpl. **(B)** Wholemounts of mutant retinas immunostained for ZO-1. Control retina is left; Dex-treated retina is right. **(C)** Number of regenerated cones in control (292.20 ± 158.11 cones) and Dex-treated retinas (522.79 ± 82.55 cones) at 21 dpl. *p=0.0010. **(D)** Immunostaining with ZPR-1 for red-green double cones in control (top) and Dex mutants (bottom) 21 dpl. Insets illustrate differences in the maturation and length of the photoreceptor outer segments. **(E)** Immunostaining for microglia using the 4C4 antibody in control (top) and Dex-treated retinas (bottom). Inserts illustrate ameboid (top) and ramified (bottom) microglia. Scale bars equal 10μm in panel A and 40μm in panels D and E.

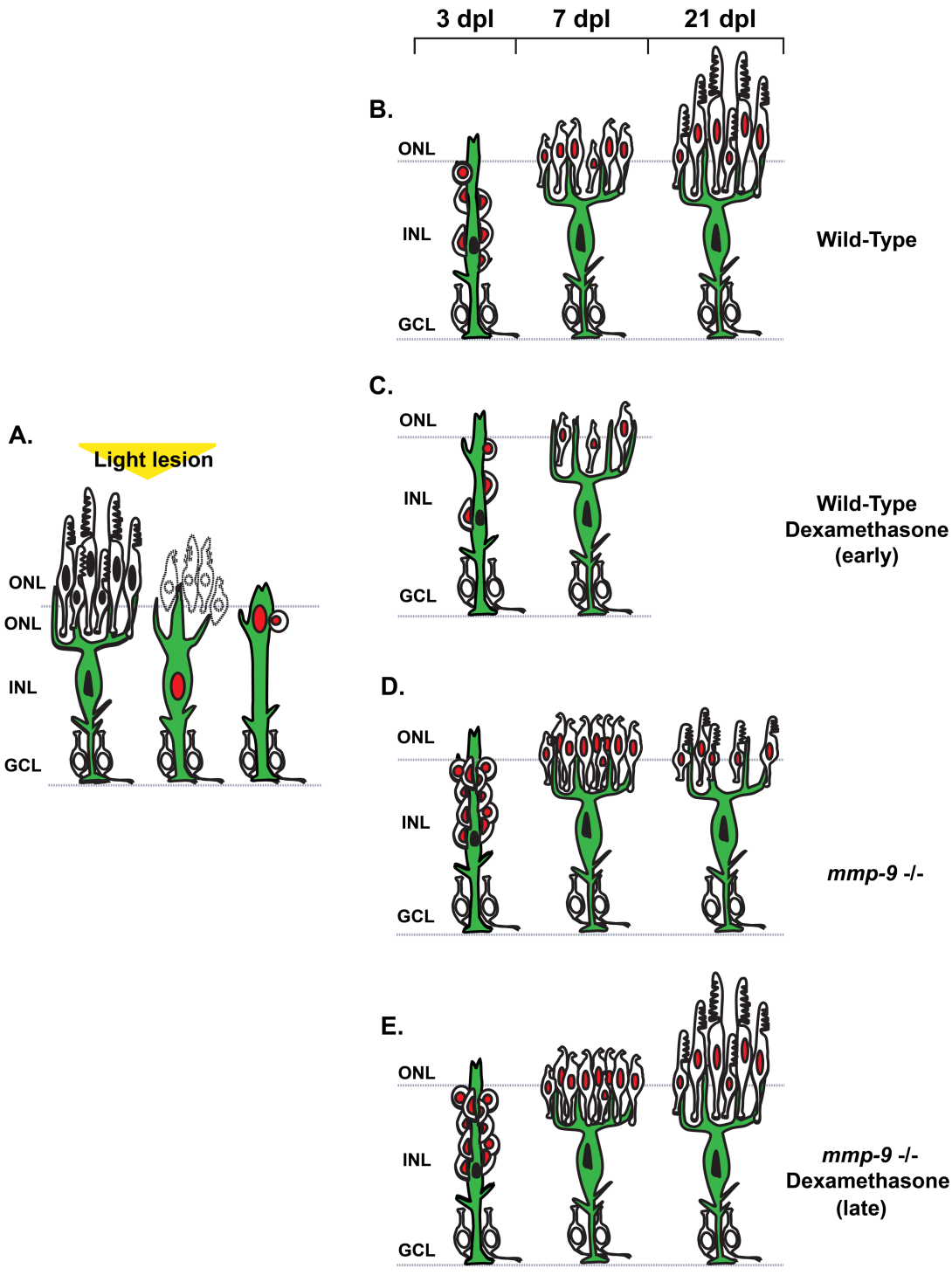

Fig 11. Summary Diagram of cone regeneration (A) Müller glia respond to photoreceptor death by expressing *mmp-9*, undergoing interkinetic nuclear migration and a single asymmetric cell division that gives rise to a neuronal progenitor. **(B)** In wild-type animals, neuronal progenitors form a neurogenic cluster around the Müller glia (3 dpl), migrate to the ONL, and differentiate into cone photoreceptors (7 dpl) that then mature (21 dpl). **(C)** Anti-inflammatory treatment results in fewer Müller gli-derived progenitors and fewer regenerated photoreceptors. **(D)** In the absence of Mmp-9, there is overproduction of Müller glia-derived progenitors and regenerating photoreceptors. However, at 21dpl, cone maturation and survival are compromised. **(E)** In the absence of Mmp-9, anti-inflammatory treatment rescues the maturation and survival of cone photoreceptors. ONL- outer nuclear layer; INL- inner nuclear layer; GCL- ganglion cell layer.

Table 1: Primer Sequences

Name	Sequence
gpia	F) 5'- TCCAAGGAAACAAGCCAAGC-3' R) 5'- TTCCACATCACACCCTGCAC-3'
mmp-9	F) 5'- TGATGTGCTTGGACCACGTAA-3' R) 5'- ACAGGAGCACCTTGCCTTTTC-3'
tnf-α	F) 5'- GCGCTTTTCTGAATCCTACG-3' R) 5'- TGCCCAGTCTGTCTCCTTCT-3'
tnf-β	F) 5'- CCTCAGACCACGGAAAAGT-3' R) 5'- GCCCTGTTGGAATGCCTGAT-3'
il-6	F) 5'- TCTTTCCCTCTTTTCCTCCTG -3' R) 5'- TCAACTTCTCCAGCGTGATG -3'
il-8	F) 5'- GTCGCTGCATTGAAACAGAA -3' R) 5'- AGGGGTCCAGACAGATCTCC-3'
nfκb1	F) 5'- ACCAGACTGTGAGCGTGAAG -3' R) 5'- CGCAAGTCCTACCCACAAGT -3'
nfκb2	F) 5'- CATATGTCCCACACAATCAAGAC-3' R) 5'- AGCCACCATAATGATCTGGAA -3'
stat3	F) 5'- GAGGAGGCGTTTGGCAAA -3' R) 5'- TGTGTCAGGGAACTCAGTGTCTG -3'

Table 2: Antibody List

Primary Antibodies	Company	Dilution
Mouse Monoclonal anti-Zn5	ZIRC; zfin.org/ZDB-ATB-081002-19	1:200
Mouse Monoclonal anti-Zpr1 (anti-Arrestin-3)	ZIRC; zfin.org/ZDB-ATB-081002-43	1:200
Mouse Monoclonal anti-Zpr-3	ZIRC; zfin.org/ZDB-ATB-081002-45	1:200
Mouse anti-HPC1	ZIRC; zfin.org/ZDB-ATB 130225-1	1:200
Mouse anti-Zrf1	ZIRC; zfin.org/ZDB-ATB-081002-46	1:1000
Mouse Monoclonal ZO-1A-12	Invitrogen 33-9100	1:200
Mouse anti-BrdU	BD Biosciences 347580	1:100
Rat anti-BrdU	Abcam 6326	1:200
Polyclonal anti-GNAT2	MBL: PM075	1:1000
Mouse Monoclonal anti-1D1 (ZF Rhodoposin)	Gift from Dr. Jim Fadool (FSU)	1:1000
Mouse Monoclonal anti-4C4 (zebrafish microglia)	Hitchcock Lab	1:200
Secondary Antibodies		
Alexa Fluor goat anti-mouse 488, 555, or 647	Invitrogen	1:500
Alexa Fluor goat anti-rabbit 488, 555, or 647	Invitrogen	1:500
Alexa Fluor goat anti-rat 488, 555, or 647	Invitrogen	1:500